Raman spectroscopy, ab-initio model calculations, and conformational, equilibria in ionic liquids

Berg, Rolf W.

Published in:
Ionic Liquids in Chemical Analysis

Publication date:
2009

Document Version
Early version, also known as pre-print

RAMAN SPECTROSCOPY, *AB-INITIO* MODEL CALCULATIONS AND CONFORMATIONAL EQUILIBRIA IN IONIC LIQUIDS

Rolf W. BERG
Department of Chemistry
Technical University of Denmark
B. 207, Kemitorvet, DK-2800 Kgs. Lyngby, Denmark

Fax: +45 4588 3136; Tel: +45 4525 2412; E-mail: rwb@kemi.dtu.dk

Keywords: Raman spectra, Molecular vibration, Spectroscopy, Molten salt, ab-initio, Ionic liquid, Review, Conformation, Crystal structure, Liquid structure, Molecular structure, Polymorphism, Rotamers, Localized structure, Conformation, Hydrogen bonds, Internal rotation, Normal modes

1. Abstract

A review of the recent developments in the study and understanding of room temperature ionic liquids are given. An intimate picture of how and why these liquids are not crystals at ambient conditions is attempted, based on evidence from crystallographical results combined with vibrational spectroscopy and *ab-initio* molecular orbital calculations. A discussion is given, based mainly on some recent FT-Raman spectroscopic results on the model ionic liquid system of 1-butyl-3-methyl-imidazolium ($[C_4C_1Im]^+X^-$) salts. The rotational isomerism of the $[C_4C_1Im]^+$ cation is described: the presence of *anti* and *gauche* conformational forms that has been elucidated in remarkable papers by Hamaguchi et al. Such presence of a conformational equilibrium seems to be a general feature of the room temperature liquids. The "localised structure features" that apparently exist in ionic liquids are described. It is

hoped that the structural resolving power of Raman spectroscopy will be appreciated by the reader, when used on crystals of known conformation and on the corresponding liquids, especially in combination with modern quantum mechanics calculations. It is hoped that these inetrdisciplinary methods will be applied to many more systems in the future. A few examples will be discussed.

I. Introduction

Generally room temperature ionic liquids (ILs) consist mostly of ions, e.g. as shown in Fig. 1 {1}. In these liquids the Coulomb interaction plays a major role, in contrast to the situation in ordinary molecular liquids where only dipolar and/or higher order multipolar electrostatic interactions occur. The long-range nature of the Coulomb force tends to make the melting points of ionic crystals much higher than for molecular crystals. The ILs are extraordinary with their low melting points and reasons for this will be considered later.

The intermolecular interactions in ionic liquids are of great importance for their general use, and the basic knowledge in the physical chemistry of these solvent systems is under intensive growth. The number of publications is rizing steeply and it is difficult to get an overview. Early studies probed the nature of interactions in so-called first-generation chloroaluminate ionic liquids {2}, and now also information becomes available for second generation, air-stable systems. Many IL studies have covered theoretical aspects {3}, {4}, {5}, {6}, {7} and X-ray crystallography of the frozen melts {8}, {9}, {10}, {11}, {12}, and solubilities of gases in ionic liquids {13}, {14}, {15}.

Hydrogen-bonding is known to occur between the cations and anions in most ionic liquids. As demonstrated by several investigators by e.g. IR and Raman spectroscopy on systems containing 1-alkyl-3-methyl-imidazolium, all three ring protons at C2, C4, and C5, see Fig. 2, form strong hydrogen bonds to halide ions, and the C2 proton is hydrogen bonded to the $[BF_4]^-$ anion in neat $[C_2C_1Im][BF_4]$ {16}. The degree of hydrogen bonding between the ring-bound hydrogen atoms and the anion seems to change significantly when going from e.g. a neat chloride to a hexafluorophosphate. IR spectroscopy has provided detailed information on the hydrogen-bonded interaction between water molecules and ionic liquids in e.g. $[C_4C_1Im][PF_6]$ and $[C_4C_1Im][BF_4]$, see {15}, {17}, {18}, {19}.

Raman spertroscopy of $[C_4C_1Im]Cl$ - $EtAlCl_2$ ionic liquids (Et = ethyl) has shown that the distribution of the ethylchloroaluminate(III) species follows a chlorobasicity pattern similar to that found in alkali chloroaluminate(III) ionic liquids {20}, {21}. Hence, in these ionic liquids Cl^- and $[EtAlC1_3]^-$ ions are

found when the liquid is chlorobasic. In moderately acidic ionic liquids, $EtAlCl_3$ and $[Et_2Al_2Cl_5]^-$ ions are present, and in highly acidic compositions $[Et_3Al_3Cl_7]^-$ and $Et_2Al_2Cl_4$ are important components. Similar results are found for $[C_2C_1Im]Cl$-Et_2AlCl ionic liquid systems {22}. Closer inspection of the Raman spectra of the acidic $[C_2C_1Im]Cl$ - $EtAlCl_2$ ionic liquids has revealed that the species $[AlCl_4]^-$, $[EtAl_2Cl_6]^-$, Et_2AlCl and $Et_3Al_2Cl_3$ are present {22}. Exchange of ethyl and chloride ligands must be taking place; a quite likely behavior for such complex mixtures.

The ILs interact with surfaces and electrodes {23}, {24}, {25}, and many more studies have been done that what we can cite. As one example, *in situ* Fourier transform infrared reflection absorption spectroscopy (FT-IRAS) has been utilized to study the molecular structure of the electrified interphase between a 1-ethyl-3-methylimidazolium tetrafluoroborate $[C_2C_1Im][BF_4]$ liquid and gold substrates {26}. Similar results have been obtained by surface enhanced Raman scattering (SERS) for 1-butyl-3-methylimidazolium hexafluorophosphate $[C_4C_1Im][PF_6]$ adsorbed on silver {24}, {27} and quartz {28}.

Mixed systems of organic molecules and ionic liquids that form separate phases (by thermomorphic phase separation) have been also studied by Raman spectroscopy {29}.

II. Brief Introduction to Raman Spectroscopy

A. Basics.

The effect of Raman scattering may be defined as instantaneous inelastic scattering of electromagnetic radiation (light) and was discovered in 1928 by Indian physicists Raman and Krishnan {30}, {31}, {32}, {33}. When a photon collides with a sample, it may be elastically scattered (called Rayleigh scattering) or an amount of energy may be exchanged with the sample (Stokes or anti-Stokes Raman processes) as shown schematically in the quantum energy level diagram in Fig. 3. Accordingly, the outgoing photon has less or more energy than the incoming one. A Raman process corresponds to a (fundamental) transition among certain group vibrational states. For the Raman spectral band to occur with a significant intensity, the molecular bond stretching or angle deformation vibration must cause a *change* in the polarizability of the molecule. The ensemble of light scattering bands constitute the

Raman spectrum. Stokes-shift Raman spectra are most often measured; i.e. the scattered photons have lower frequency than the incident radiation.

Dramatic improvements in instrumentation (lasers, detectors, optics, computers, etc) have during recent years raised the Raman spectroscopy technique to a level where it can be used for "species specific" quantitative chemical analysis. Although not as sensitive as e.g. infrared absorption, the Raman technique has the advantage that it can directly measure samples inside ampoules and other kinds of closed vials because of the transparency of many window materials. Furthermore, with the use of polarization techniques, one can derive molecular information that cannot be obtained from infrared spectra. Good starting references dealing with Raman spectroscopy instruments and lasers are perhaps {34}, {35}, {36}, {37}, {38}.

Raman and Infrared spectroscopies are closely interrelated in that they both depend on characteristic "*group*" molecular motions in the sample that give rise to the vibrational bands in the spectra. As an example, bands occurring near 2950 cm^{-1} can often be assigned to aliphatic C-H stretching transitions (although sometimes in "Fermi-resonance" with overtones and other nonfundamental transitions). So-called empirical group frequency charts are available, specifying "fingerprint" bands, that may be used to identify pure materials or the presence of a particular component in a mixture, see e.g. {39}, {40}, {41} and {42}.

During the IR absorption process, a quantum of radiation (a photon) of a particular energy E and with a frequency ν ($E = h\nu$) is absorbed (h is Planck's constant). During the absorption the molecular system undergoes a transition from the ground state (quantum number $v = 0$) to an excited state ($v = 1$), in the present case e.g. corresponding to a CH_3 group C-H bond stretching with a wavenumber shift of 2900 cm^{-1}. In contrast to this, during Rayleigh and Raman scattering, an exiting photon of much higher energy hits the molecular system and raises it to a virtual state, from where it "immediately" falls back. There are two possibilities, here illustrated with green Ar^+ light of 514.5 nm wavelength corresponding to 19435 cm^{-1}. In so-called Stokes Raman scattering (not so likely), the system falls back to the $v = 1$ state (emitting a 16535 cm^{-1} photon), or in Rayleigh scattering (more likely) to the $v = 0$ ground state

(emitting light at ~19435 cm^{-1}), producing the so-called Rayleigh wing). If the system is starting from the v = 1 state (not so likely at room temperature because of the Boltzman distribution), similar transitions can happen. Now also a so-called anti-Stokes Raman process is possible producing photons at 22335 cm^{-1}. Most Raman spectroscopy studies report data corresponding to Stokes Raman transitions. Samples (or impurities therein) having energy states near the "virtual" ones (here at e.g. ~19435 cm^{-1}) may absorb photons from the incident light and later re-emit the light as a broad intensive background called *fluorescence*.

Although similar transitional energy ranges occur in IR and Raman spectroscopy, different selection rules govern the intensities in Raman scattering and IR absorption spectra. Hence both types of spectra are often required to fully characterise a substance: A necessary requirement for a molecular motion (such as a vibration, rotation, rotation/ vibration, or lattice normal mode) to be measurable in IR spectra it is needed that an oscillating dipole moment is produced during the vibration (in Raman the motion within the molecular system should vary the polarizability). Combinations, differences or overtones of these transitions can occur, but normally only weakly. The selection rules of the transitions are described in quantum mechanics and group theory, see e.g. {31}, {32}, {33}, {43} and {44}.

B. Experimental, fluorescence and FT-Raman spectroscopy instrumentation.

Applications of Raman spectroscopy in analytical chemistry have been limited by the presence of fluorescence from some samples (or from some impurities in the samples). In case of strong fluorescence the use of less-energetic near-IR lasers for the excitation is often a requirement. Fourier-transform Raman instruments have been developed, that successfully apply e.g. ~1064 nm laser excitation (from solid state Nd-YAG or Nd-YVO_4 lasers) to avoid the fluorescence {45}. The advantage of Raman spectroscopy over IR and other analytical techniques (when the fluorescence problems can be circumvented) stems from the ability of Raman to identify discrete species *in situ*. Raman spectra can be obtained directly from samples of any phase, in e.g. glass cells. With a minimum effort, temperature and pressure limitations can be overcome. The polarization properties of the Raman

scattered light may be employed to select only the isotropic intensity of the symmetric vibrational modes, thereby helping conclusive assignment of the spectra.

The Raman effect is weak, perhaps only 10^{-8} of the photons hitting the sample are scattered in Raman. The use of high power lasers (to circumvent the low scattering efficiency) often results in sample decomposition, and fluorescence interference from impurities must be considered a likely problem for visible light. Recent development of charge coupled detectors (CCDs) and notch filters have revolutionized the Raman technique for samples that do not emit much fluorescence. Sampling through a microscope - under high magnification - is an effective way to collect Raman light over a large solid angle, and then only minute sample quantities are necessary.

Room temperature ionic liquids have been the object of several Raman spectroscopy studies but often ILs emit intensive broad fluorescence. In our own experiments, the use of visible laser light (green 514.5 nm or red 784 nm) resulted in strong fluorescence {29}, {46}. Similar observations have been reported for many IL systems. Our experimental spectra needed to be obtained by use of a 1064 nm near-infrared exciting source (Nd-YAG laser at 100 mW of power). The scattered light was filtered and collected in a Bruker IFS66-FRA-106 Raman Fourier-Transform spectrometer equipped with a liquid-N_2 cooled Ge-diode detector. Samples were in small glass capillary tubes at ~23ºC. The spectra were calculated by averaging ~200 scans followed by apodization and fast-Fourier-transformation to obtain a resolution of ~2 cm^{-1} and a precision better than 1 cm^{-1}. The spectra were not corrected for (small) intensity changes in detector response versus wavelength.

III. Brief Introduction to *ab-initio* Model Calculations

Ab-initio and semi-empirical Molecular Orbital (MO) model calculations have become an efficient way to predict chemical structures and vibrational (i.e. Raman scattering and IR emission) spectra. We and others have used such approaches to better understand certain features of the spectra, as explained in the following. The basic principles underlying *ab-initio* model calculations have been described in

many textbooks and papers, see e.g. {44}, {47}, {48}. Applications in relation to ILs and similar systems have also been reported, as discussed later.

The MO calculations may nowadays be performed with e.g. the GAUSSIAN 03W program package {49}. A guessed molecular geometry (conformation) is used as input together with some kind of approximation to the atomic orbitals (so-called basis sets, often sums of Gaussian functions). The total energy is minimized by restricted Hartree-Fock (RHF), Møller Plesset (MP2) or Density Functional Theory (DFT) principles, using e.g. third order Becke-Lee-Yang and Parr (B3LYP) procedures {44}, {48}, {49}. Common basis sets are the split valence 6-31+G(d,p) sets including diffuse orbitals (d) augmented with Pople's polarization functions (p) {49}. The molecular ions are commonly assumed to be in a hypothetical *gaseous free state* and without any pre-assumed symmetry, but some calculations also involve better approximations to real systems. After optimization, giving a geometry with a minimum energy – perhaps not a global one - vibrational frequencies and intensities (spectra) and eigenvectors for the normal modes are calculated and displayed on a computer screen, to identify the dominating motions. The frequencies (wavenumbers) are correlated with the Raman and IR bands.

The calculated and experimental vibrational spectra are in more or less good agreement. The wavenumber scale is often calculated as slightly too high, due to the lack of good modelling of the orbitals and interactions with the surroundings. In the gas phase empirical scale factors of ~0.95 are sometimes used to get fairly accurate wavenumber fits. A scaling factor of 1 was used in this work.

IV. Case Study on Raman Spectroscopy and Structure of Imidazolium-based ILs

As mentioned above, vibrational spectroscopy is known to be a very powerful tool in the study of molecular stuctures and interionic interactions in ILs {18}, {19}, {50}. This is especially so when done in combination with crystal structure studies, as explained in the following.

To illustrate the situation, we start our discussion with the example of the alkyl-methylimidazolium liquids, from $[C_2C_1Im]^+$ to $[C_{18}C_1Im]^+$, and a number of different anions. Although other techniques

such as infrared spectroscopy, X-ray and neutron diffraction studies have been used to study these ions in the liquid or solid state or at surfaces {12}, {51}, {52}, {53}, {54}, {55}, {56}, {57}, {58}, {59}, {60}, {61}, a real gain in our understanding came with the combination of crystal structure solution, Raman spectroscopy and ab-initio DFT calculations {50}, {62}. We concentrate the story on the instructive example of the l-butyl-3-methylimidazolium cation, $[C_4C_1Im]^+$ (see Fig. 2, without carbon atoms 11 and 12), that makes a number of ILs with varying properties, depending on the different anions. The two prototype ILs $[C_4C_1Im][BF_4]$ and $[C_4C_1Im][PF_6]$ have already been used extensively in fundamental investigations as well as in practical applications. Therefore, the elucidation of their crystal and liquid structures were an important first step for the understanding of ILs in general {50}.

The most fundamental question about ILs to be discussed is: Why are ILs liquids at the ambient temperature, despite the fact that they are composed solely of ions? This question can be answered as described in the following.

$[C_4C_1Im]Cl$ and $[C_4C_1Im]Br$ are crystals at room temperature, while $[C_4C_1Im]I$ is a IL (melting point -72°C {63}). A typical ionic crystal such as NaI only melts at ~660ºC. By cooling $[C_4C_1Im]Cl$ and $[C_4C_1Im]Br$ liquids below their melting points, supercooled liquids are easily obtained. Crystals could be grown of the $[C_4C_1Im]Cl$ and $[C_4C_1Im]Br$ salts and X-ray diffraction used to determine the crystal structures. These systems thus comprised unique systems for studying the structure of the $[C_4C_1Im]^+$ cation in the liquid and crystalline states.

A crystal polymorphism was discovered in the $[C_4C_1Im]Cl$. It adopts a monoclinic (m.pt. ~41 °C) and an orthorhombic (m.pt. ~66 °C) crystal structure {57}, {58}, {64}, {65}. In the following, we use the Hamaguchi notation ”Crystal (1)” and ”Crystal (2)”. The crystal structures were determined by X-ray diffraction of $[C_4C_1Im]Cl$ ”Crystal (1)” and [C4C1Im]Br at room temperature {57} and independently, of $[C_4C_1Im]Cl$ ”Crystal (1)” and ”Crystal (2)”, as well as that of $[C_4C_1Im]Br$ at -100° C {58}. The structures determined by different authors agreed quite well with each other, taking into account that the lattice constants vary with temperature. The molecular structure of the $[C_4C_1Im]^+$ cation in

$[C_4C_1Im]Cl$ ”Crystal (2)” is different from that in (1) but it was the same as that in $[C_4C_1Im]Br$, as also proved later by the Raman spectra.

The $[C_4C_1Im]^+$ cations in the two polymorphs were found predominantly to differ with respect to conformation: The structural results showed that the polymorphism is due to a rotational isomerism of the butyl group of the $[C_4C_1Im]^+$ cation around C7-C8, as defined in Fig. 2. In the monoclinic polymorph, the butyl chain is in *anti* (or *trans*) conformation around C7-C8, and in the orthorhombic polymorph it is *gauche* around C7-C8. The conformational difference reveals itself in the rotation of the butyl chain around the C7-C8 bond, that differed by 106.16° between the two conformers {58}. The C8-C9 conformation was found to be *anti* in both polymorphs. In a convenient and obvious notation, these two conformers of the $[C_4C_1Im]^+$ cation are *here* referred to as the AA and the GA forms (Hamaguchi et al. denote them TT and GT). Also the crystal structure of $[C_4C_1Im]Br$ has been reported {58}.

The crystal structure of the monoclinic $[C_4C_1Im]Cl$ ”Crystal (1)” is shown in Fig. 4. Details of structural data are available from the Cambridge Crystallographic Data Centre {66}. The crystal belongs to space group $\boldsymbol{P}2_1/n$ with $\boldsymbol{a}$ = 9.982(10), $\boldsymbol{b}$ = 11.590(12), $\boldsymbol{c}$ = 10.077(11) Å, and $\boldsymbol{\beta}$ = 121.80(2)°. Both the $[C_4C_1Im]^+$ cations and the chloride anions form separate columns extending along the crystal $\boldsymbol{a}$ axis. The imidazolium rings are all planar pentagons. The stretched *n*-butyl group of the $[C_4C_1Im]^+$ cation takes a *anti-anti* (AA) conformation with respect to the C7-C8 and C8-C9 bonds, as shown in the inset of Fig. 4. The butyl groups stack together (aliphatic interaction) and form columns extending along the $\boldsymbol{a}$ axis, in which all the imidazolium ring planes are parallel with one another. Two types of cation columns with different orientations exist, the planes of the imidazolium rings in the two different columns making an angle of 69.5°. Zig-zag chains of Cl^- anions directed in the $\boldsymbol{a}$ direction are accommodated in channels formed by four cation columns, of which two opposite columns have the same orientation. The three shortest distances between Cl^- anions in the zig-zag chain were 4.84 Å, 6.06 Å and 6.36 Å and these distances are much larger than the sum of the van der Waals radii of Cl^- (3.5 Å). There seems to be no specific interaction among the Cl^- anions, and they are likely to be

aligned under the effect of Coulombic forces. The chloride ion is very close to the hydrogen H2 in the ring (2.55 Å), and to the two methylene protons on C7 (2.72 and 2.73 Å) {57}, {58}, meeting the criteria for relatively strong hydrogen bonds {67}, {68}. Similarly strong hydrogen bonds are observed in the orthorhombic form {58}. Also other crystal structures e.g. of the 1-ethyl-3-methylimidazolium chloride ($[C_2C_1Im]Cl$) {15}, the tetrafluoroborate ($[C_2C_1Im][BF_4]$) and other salts {69} have been reported.

The crystal structure of orthorhombic $[C_4C_1Im]Br$ (m.pt. 77.6ºC {65}) is shown in Fig. 5. The detailed structural data are available from the Cambridge Crystallographic Data Centre {66}. The [C4C1Im]Br crystal belongs to the space group ***Pna2₁*** with ***a*** = 10.0149(14), ***b*** = 12.0047(15), ***c*** = 8.5319(11) Å. As for the $[C_4C_1Im]Cl$ "Crystal (1)", the cations and anions form separate columns extending along the ***a*** axis. In $[C_4C_1Im]Br$ the *n*-butyl group takes a *gauche-anti* (GA) conformation with respect to the C7-C8 and C8-C9 bonds (see inset of Fig. 5). Only one kind of cation column is found. The imidazolium rings are stacked so that the N-C-N moiety of one ring interacts with the C=C portion of the adjacent ring. The adjacent ring plane can be obtained by rotation of the ring by about 73° around an axis involving the two N atoms. The zig-zag chain of Br^- anions resides in the channel produced by four cation columns, extending in the ***a*** direction. The shortest three Br^--Br^- distances (4.77, 6.55, and 8.30 Å) are all longer than the sum of the van der Waals radii (3.7 Å). This indicates that there is no specific interaction among the Br^- anions and that the zig-zag molecular arrangement is a result of Coulombic interactions.

V. Raman Spectra and Structure of $[C_4C_1Im]^+$ Liquids

The information obtained from the study of the $[C_4C_1Im]^+$ crystals can be used as a basis to better understand the liquid structure of the $[C_4C_1Im]X$ ionic liquids (X is an anion). It is well-known that Raman spectroscopy facilitates comparative studies of the structures in crystals and liquids. Raman spectra of $[C_4C_1Im]Cl$ "Crystals (1) and (2)", and $[C_4C_1Im]Br$ by Hamaguchi et al. {50}, {57}, {59}, {64}, {70} are shown in Fig. 6. As seen, the two polymorphs of $[C_4C_1Im]Cl$ gave distinct Raman spectra differing considerably, while those of $[C_4C_1Im]Cl$ "Crystal (2)" and $[C_4C_1Im]Br$ were almost

identical. These findings are consistent with the X-ray diffraction experimental results. The halogen anions are inactive in Raman scattering - except for the lattice vibrations, that are observed in the wavenumber region below 200 cm^{-1} {71}. Therefore, all the Raman bands seen in Fig. 6 can be ascribed to the $[C_4C1Im]^+$ cation. Fig. 6 was accordingly interpreted to indicate that the $[C_4C_1Im]^+$ cation takes two different conformations in those salts. To be in accordance with the X-rays results, at least the cation must adopt the same molecular conformation in $[C_4C_1Im]Cl$ "Crystal (2)" and $[C_4C_1Im]Br$, and a different one in $[C_4C_1Im]Cl$ "Crystal (1)". In this way it emerged that the Raman spectral differences in Fig. 6 most likely originated from the rotational isomerism around the C7-C8 (the AA and GA isomerism) of the butyl chain of the $[C_4C_1Im]^+$ cation {64}, {70}.

Raman spectra of liquid $[C_4C_1Im]X$ (X = Cl, Br, I, $[BF_4]$, $[PF_6]$) measured at room temperature are shown in Fig. 7. The spectra of $[C_4C_1Im]Cl$ "Crystal (1)" and $[C_4C_1Im]Br$ are also included for reference purposes. Spectra for fluids $[C_4C_1Im]Cl$ and $[C_4C_1Im]Br$ were taken from supercooled liquids. The Raman spectra of the $[C_4C_1Im]X$ liquids were surprisingly alike. One should note that the Raman spectral bands of the separate $[BF_4]^-$ and $[PF_6]^-$ anions - that are already well known {41} - have been *deleted in Fig.7*. However, from the similarity of the spectra it seems that the structural properties of the $[C_4C_1Im]^+$ cation in these liquids are very similar. But what else can be deduced from the spectra?

VI. Normal Mode Analysis and Rotational Isomerism of the $[C_4C_1Im]^+$ Cation

To pursue this question further, Ozawa et al. {70} have performed density functional calculations (DFT) with Gaussian98 at the B3LYP/6-31G+** level. In the calculation, the structures of the AA and GA forms of $[C_4C_1Im]^+$ were optimized in the vicinity of the determined X-ray crystal structures for $[C_4C_1Im]Cl$ "Crystal (1)" and $[C_4C_1Im]Br$, respectively. The structures of the optimized $[C_4C_1Im]^+$ cations in the two crystals are depicted in Fig. 8, together with the experimental spectra (in a limited wavenumber region of 1000-400 cm^{-1}). The calculated fundamental frequencies and intensities were

included in Fig. 8 as thick vertical bars. As seen the calculated “bar”-spectra reproduced the observed spectra quite well.

The normal mode calculation was used to elucidate the rotational isomerization equilibrium of the $[C_4C_1Im]X$ liquids. In the wavenumber region near 800-500 cm^{-1}, where ring deformation bands are expected, two Raman bands appeared at ~730 cm^{-1} and ~625 cm^{-1} in the $[C_4C_1Im]Cl$ ”Crystal (1)”. In the $[C_4C_1Im]Br$ these bands were not found. Here instead, another couple of bands appeared at ~701 cm^{-1} and ~603 cm^{-1}. To assist the interpretatation of the spectra, the normal modes of vibrations calculated by Hamaguchi et al. {50} are shown in Fig. 9. It shows modes for the $[C_4C_1Im]^+$ ion of the geometry of $[C_4C_1Im]Cl$ ”Crystal (1)” at 735 cm^{-1} and 626 cm^{-1}; and similarly the modes for $[C_4C_1Im]Br$ occurring at 696 cm^{-1} and 596 cm^{-1}. Obviously the 626 cm^{-1} band of $[C_4C_1Im]Cl$ ”Crystal (1)” and the 596 cm^{-1} band of $[C_4C_1Im]Br$ originate from similar kind of *ring* deformation vibrations, but they have different magnitudes of the coupling with the CH_2 rocking motion of the C8 carbon (encircled in Fig. 9). It thus seems that more intensive coupling occurs between (i) the CH_2 rocking motion and (ii) the ring deformation vibrations in the GA form (596 cm^{-1}) than in the AA form (626 cm^{-1}), resulting in an overall lower frequency of the mode and therefore a lower wavenumber position of the Raman band {50}.

By comparing their normal coordinate analysis results and their *liquid* experimental Raman spectra in Fig. 7, Hamaguchi et al. {50}, {57}, {59}, {64}, {70} concluded that the two rotational isomers AA and GA must coexist in the ionic liquid state (AA and GA were called TT and GT by Hamaguchi et al.). According to the Raman spectra of all the liquids in Fig. 7, both of the key bands for the AA conformer (625 cm^{-1} and 730 cm^{-1} bands), and for the GA conformer (the 603 cm^{-1} and 701 cm^{-1} bands), respectively, appeared in the spectra. Therefore, the two isomers of rotational freedom around the C7-C8 and C8-C9 bonds - anti-anti and gauche-anti – must coexist in these $[C_4C_1Im]X$ liquids.

Furthermore, the observed relative intensity of the 625 cm^{-1} band to that of the 603 cm^{-1} band should be correlatable with the AA/GA population ratio of the conformation equilibruim. The observed ratios

depended slightly on the anion: For the halides, it seems to increase in the order $[BF_4]^- \approx [PF_6]^- \approx Cl^- < Br^- < I^-$ {50}.

During our work on $[C_4C_1Im]^+$ and $[C_6C_1Im]^+$, we have repeated the experiments and calculations for the $[C_4C_1Im]^+$ cation and found the results of Hamaguchi et al. to be essentially reproducible (details explained in ref. {46}). Our calculated Raman spectra in the whole range for the AA (anti-anti) and GA (gauche-anti) conformers of $[C_4C_1Im]^+$ are shown in Fig. 10 and 11. Our assignments (approximate descriptions of the modes giving origin to the Raman bands) are listed in Table 1, based on the calculated vibrational frequencies and we communicate the intensities of the infrared and Raman bands. The movements were depicted on a PC-screen and assignments were derived using the Gaussian03W software.

Our recalculated modes of the $[C_4C_1Im]^+$ cation were obtained with somewhat higher frequencies: the modes at 626, 735, 596 and 696 cm^{-1} by Hamaguchi et al. in Fig. 9 became 636 and 749 cm^{-1} for our AA and 622 and 713 cm^{-1} for our GA modes, see Fig. 12.

According to the calculated minimum energy E_e of the conformers, the GA was more stable than the AA conformer, but at 298.15 K the *Gibbs* energy of the AA conformer was 0.168 kJ mol^{-1} less than that of the GA conformer, indicating 52% of *anti-anti* versus 48% of *gauche-anti* or almost equal amounts of the two conformers at equilibrium at room temperature {46}. A higher difference between the AA and GA energy was found in other calculations {73}. These results are consistent with the observation of both conformers being simultaneously present in the spectra of the $[C_4C_1Im]^+$ liquids as observed by Ozawa et al. {70}, see Fig 7.

Our obtained experimental Raman signals for the $[C_4C_1Im]^+$ cation liquids are given in Fig. 13 and the assignments are specified in Table 2, based on the calculations, some of which are summarized in Table 3. Note that bands from the $[PF_6]^-$ and $[BF_4]^-$ anions are visible, $\nu_1([PF_6]^-)$ symmetric stretching at 741 cm^{-1}, $\nu_2([PF_6]^-)$ stretching at 568 cm^{-1}, $\nu_5([PF_6]^-)$ symmetric bending at 471 cm^{-1}, $\nu_1([BF_4]^-)$

symmetric stretching at 766 cm^{-1} and $\nu_4([BF_4]^-)$ bending at 522 cm^{-1} {72}. Similar kind of experimental and calculational results for $[C_nC_1Im]X$ liquids were obtained by Carper and others {74}, {75}, {76}, {77}, {78}.

To conclude the situation for $[C_4C_1Im]^+$, Ozawa et al. {50}, {70} have discovered - by the combined use of X-ray crystallography, Raman spectroscopy, and DFT calculations - that

- one can use certain Raman bands as key bands to probe the conformation around the C7-C8 bond of the $[C_4C_1Im]^+$ cation.
- the calculated bands at ~626-636 cm^{-1} and ~735-749 cm^{-1} are characteristic of the AA conformer (*anti-anti* conformation around the C7-C8 bond), as compared to the experimental values of ~624 and ~730 cm^{-1} (Table 2), whereas the ~596-604 cm^{-1} and ~696-713 cm^{-1} calculated bands are characteristic of the GA conformer (*gauche-anti* conformation). Furthermore a characteristic frequency was calculated as ~504, (Table 1), as compared to the experimental values of ~500, ~602, and ~699 cm^{-1} (Table 2).
- experimentally the Raman spectral bands are occurring at easily recognizable peak positions and with intensities obtainable from *ab-initio* DFT calculations. Bands measured by Ozawa and Hamaguchi at 701, 625, 603, and 500 cm^{-1} correspond within experimental error to our $[C_4C_1Im][PF_6]$ liquid bands at 698, 624, 601, and 498 cm^{-1} (Table 2).

In a more refined gas phase ion pair model aimed at understanding the interaction in the $[C_4C_1Im][PF_6]$ liquid, Meng et al. {5} in a combined spectroscopic, semi-empirical and *ab-initio* study, observed hydrogen bonding between the $[PF_6]^-$ ion and the hydrogen atom at C2 in the aromatic ring of the $[C_4C_1Im]^+$ cation. Virtually identical theoretical results were obtained using both Hartree-Fock (HF) and Density Functional Theory (DFT). The DFT minimized structure is shown in Fig. 14. Obviously Meng et al. {5} have reached an *anti-gauche* (AG) conformation that probably just is local but not a global minimum. The hydrogen bonding has previously been detected by ^{13}C NMR relaxation studies on $[C_4C_1Im][PF_6]$ and related systems in the liquid state {5}, {6}, {75}, {76}.

It is well known that hydrogen bonding significantly supports the formation of ion pairs (and even higher aggregates) in electrolyte solutions when compared to systems without specific interactions. Hanke et al. {4} in another simulation study found that the largest probability for finding an anion is near C2 below and above the ring. Most likely dimeric and tetrameric ion pairs and higher aggregates are formed with a type of layer structure, in which the anions are located mainly above and below the aromatic ring near C2 {5}, {6}. The occurrence of hydrogen bonding in addition to the Coulombic interactions was put forward to explain the quite high viscosity and other specific macroscopic properties of the $[C_4C_1Im][PF_6]$ ionic liquid.

VII. Other Studies on $[C_nC_1Im]^+$ Liquids

Measured IR and Raman spectra of a series of 1-*alkyl*-3-methyl-imidazolium halides and hexafluorophosphate ionic liquids ($[C_2C_1Im][PF_6]$ to $[C_4C_1Im][PF_6]$) were correlated with results of *ab-initio* DFT calculations at the 6-31+G* and 6-311+G(2d,p) levels {73}, {74}. It was suggested that common Raman C-H stretching frequencies in these liquids may serve as possible probes in studies of ionic interactions. Hydrogen bonding interactions were observed between the fluorine atoms of the $[PF_6]^-$ anion and the C2 hydrogen on the imidazolium ring, and between $[PF_6]^-$ anion and the H atoms on the adjacent alkyl side chains. There are at least four discernible strong vibrations in the 2878 to 2970 cm^{-1} region of the $[C_2C_1Im][PF_6]$ Raman spectrum {74}. These Raman vibrations are represented by the calculated vibrations in the 3153 to 3220 cm^{-1} region and represent a complex combination of multiple stretching and bending vibrations. The weak Raman bands observed at 3116 and 3179 cm^{-1} were assigned to vibrations associated with the imidazolium ring (H-C-C-H and N-(C-H)-N) C-H stretches.

Similar studies were done on $[C_2C_1Im][BF_4]$ and other 1-ethyl-3-methylimidazolium liquid salts {16}, {69}, {79}, {80}. In the Raman spectral range 200-500 cm^{-1}, Umebayashi et al. {80} for liquids

containing $[BF_4]^-$, $[PF_6]^-$, $[CF_3SO_3]^-$, and $[(CF_3SO_2)_2N]^-$ found bands at 241, 297, 387, 430, and 448 cm^{-1} that must originate from the $[C_2C_1Im]^+$ ion. However, the 448 cm^{-1} band could not be reproduced by theoretical calculations in terms of a single given $[C_2C_1Im]^+$ conformer. The ethyl group bound to one N atom of the imidazolium ring is able to rotate around the C-N bond to yield two different torsion conformers, see Fig. 15. The energy barrier of this rotation was calculated with an energy amplitude of ~2 KJ mol^{-1} {80}. Two local minima were found, suggesting that the two conformers can be present in equilibrium. Full geometry optimizations followed by normal frequency analyses indicated that the two conformers of minimum energy were those with planar and nonplanar ethyl groups against the imidazolium ring plane, and that the nonplanar conformer was the most favorable. The Raman bands at 241, 297, 387, and 430 cm^{-1} were found to mainly originate from the nonplanar conformer, whereas the 448 cm^{-1} band originated from the planar conformer. Indeed, the enthalpy for conformational change from nonplanar to planar $[C_2C_1Im]^+$, obtained experimentally by analyzing band intensities of the conformers at various temperatures, was practically the same as the enthalpy evaluated by the theoretical calculations. We thus conclude that the $[C_2C_1Im]^+$ ion exists as planar or nonplanar conformers in equilibrium in its liquid salts {80}, and this was confirmed by X-ray diffraction {69}. For the longer chain $[C_nC_1Im]^+$ systems also non-planar forms are most stable, e.g. compare with the AA and GA conformers of $[C_4C_1Im]^+$ in Fig. 9.

We have shown {46} that the same situation as for $[C_4C_1Im]^+$ exists for longer alkyl chain systems, at least for the 1-hexyl-3-methylimidazolium cation. Raman spectra for $[C_6C_1Im]^+$ cation systems have bands at 698, 623, and 601 cm^{-1}(but no distinct band at ~498 cm^{-1}). A comparison between typical experimental spectra is shown in Fig. 16. Also the calculations came out in much the same way, as can be seen by comparing the results in Fig. 17 with those from Fig. 11 (insets).

All in all, it was recognised, both from spectra and calculations that the characteristic frequencies do not change significantly when the butyl group was exchanged for a hexyl group, and we conclude that the AA - GA isomerism phenomenon probably is general, and not specific to the $[C_4C_1Im]X$ ionic liquids. For a discussion of the hexyl systems we refer to our comprehensive report {46}.

VIII. Conformations Equilibria in Liquids *versus* Temperature

The Raman spectra of $[C_nC_1Im][BF_4]$ from n = 10 to n = 2 in the liquid state at room temperature are shown in Fig. 18. Clearly the rotational isomerism around C7-C8 interconvert the AA and GA conformers so as to change the AA/GA ratio with the cation. For $[C_2C_1Im][BF_4]$ there can be no rotational isomerism around C7-C8 because C8 is the end methyl group {16} and only one Raman band is observed at 596 cm^{-1}, corresponding to the band from the GA conformation of $[C_4C_1Im][BF_4]$. This observation was rationalized by Hamaguchi et al. {50} who noted that the methyl rocking motion of the C8 carbon is strongly coupled to the ring deformation vibration and pushes down the frequency in $[C_2C_1Im]^+$ exactly as in the case of the GA conformation of the $[C_4C_1Im]^+$ cation.

For longer side-chains, the 625/ 603 cm^{-1} Raman intensity ratio increases with increasing n because the *all*-anti AA..... kind of band at 625 cm^{-1} grows in intensity. Since the vibrational modes are very similar - being localized within the imidazolium ring and around the C7 and C8 carbons (see Fig. 12) - their Raman cross sections are thought to be quite independent of the chain length {46}. Therefore, the 625/ 603 cm^{-1} Raman intensity ratio can be regarded as a direct measure of the AA.../GA... isomer ratio. The observed *increase* of the 625/603 cm^{-1} intensity *ratio* with n means that the AAA.../GAA... isomer ratio increases as the chain becomes longer. The AAA... structure stabilization relatively to the GAA... one for longer alkyl chains is understandable only if we assume interactions among the cations. Otherwise, the relative stability would be determined alone by the energy difference between the *anti* and *gauche* conformations around the C7-C8 bond and would be likely to be independent of the chain length. Instead, the AA.../GA... ratio dependence of the chain-length therefore must depend on aliphatic interactions between the alkyl chains. In Fig. 18, the broad CH_2 rocking and bending features observed for longer-chain $[C_nC_1Im][BF_4]$ liquids (n = 7-10) in the region near 800-950 cm^{-1}, are indicative of such interactions between the alkyl chains {50}, similar to the interactions found for certain meso-phase liquid crystals when n > 12, see {12}, {55}, {81}.

An unusually long equilibration time has been observed upon melting of a single crystal of the AA polymorph of $[C_4C_1Im]Cl$ "Crystal (1)" heated rapidly from room temperature to 72°C to form a droplet of liquid in a non-equilibrium state {50}. Raman versus time spectra are reproduced in Fig. 19. Before melting and for some time after only the band at 625 cm^{-1} of the AA $[C_4C_1Im]^+$ cation was observed in the 600 to 630 cm^{-1} region. Gradually 603 cm^{-1} band due to the GA conformer became stronger. After about 10 min. the AA/GA intensity ratio became constant. The interpretation {50} is that the rotational isomers do not interconvert momentarily at the molecular level. Most probably it involves a conversion of a larger *local structure* as a whole. The existence of such local structures of different rotamers has been found by optical heterodyne-detected Raman-induced Kerr-effect spectroscopy (OHD-RIKES) {82}, Coherent anti-Stokes Raman scattering (CARS) {83}, neutron scattering and diffraction experiments {54}, {53}, and by theoretical molecular dynamics calculations {4}, {7}, {84}, {85}.

The enthalpy difference between the AA and GA conformers in the 1-butyl-3-methylimidazolium tetrafluoroborate ILs is much smaller than the corresponding enthalpy difference between the conformers of a free butane chain. This indicates that the l-butyl-3-methylimidazolium cations most likely form *local liquid structures* specific to each rotational isomers {50}. Coexistence of these local structures - incorporating different rotational isomers - seems to hinder the crystallization. This is probably the reason for the low melting points of such ILs.

These local structures most probably distinguish ILs from conventional molecular liquids and may explain why ILs phases are between a liquid and a crystal.

IX. Local Structures in Ionic Liquids

From NMR spectroscopy it is known that conformational isomers of alkane chains give coalesced peaks indicating transformation between the conformers taking place much faster than a second. Accordingly, one should expect single $[C_4C_1Im]^+$ cations undergoing AA to GA transformation almost

instantaneously {86}. The observed ~10 min. long equilibration time in liquid $[C_4C_1Im]Cl$ (Fig. 19) therefore has been taken to indicate that the conformers do not transform *at the single molecular level* but only interconvert through slow collective transformations of *ensembles* of $[C_4C_1Im]^+$ cations (analogous to a phase transition) {50}, {86}. Most probably the two rotational isomers are incorporated in specific local structures tending to interconvert only through conversion of the local structures *as a whole* and giving rize to wide pre-melting ranges and other features {65}.

The ordering of the anions in ionic liquids has - for the case of $[C_4C_1Im]I$ - been confirmed by large-angle x-ray scattering experiments {59}. In this way it seems that the zig-zag chains found in the $[C_4C_1Im]X$ crystals do exist in the ionic liquid state as well, at least partially. Thus, by combining Raman spectroscopy with several other experimental and theoretical techniques, Hamaguchi and coworkers have come to mean that both the cations and anions in $[C_4C_1Im]X$ ILs might have local ordering of their structures. Their conceptual structure of ionic liquids is reproduced in Fig. 20.

According to the model, the supposed local structures are positioned and oriented randomly, and there seeems to be no translational and orientational order at the macroscopic level. The local structure modelling of Ozawa and Hamaguchi for the $[C_4C_1Im]X$ ILs is shown in Fig. 20 (e) in comparison with the structures of a crystal (a), liquid crystals (b and c), and a conventional liquid (d). In the crystal (a), component molecules or ions are arranged to form a periodic lattice with long-range order. In a standard liquid state (d), the molecules or ions take random positions and random orientations and there is no order. In liquid crystals (b and c), different kinds of long-range order exist, with e.g. only partial orientational order (b) or random position (c).

In $[C_4C_1Im]X$ ILs, the supposed ”local structures” are positioned and oriented randomly, and there seeems to be no translational and orientational order at the macroscopic level. Taking into account that the $[C_4C_1Im]X$ ILs are all transparent (not opaque), the dimension of those “local structures” must be much smaller than the wavelength of visible light (<100 Å) {50} {86}.

Microphase segregation in imidazolium-based ionic liquids has also been discussed, and the existence of polar and nonpolar microsegregated domains in ionic liquids has been predicted in molecular simulation dynamics {87}. The structural analysis helps the understanding of solvation of nonpolar, polar, and associating solutes in these media {53}, {87}. The existence of an extended hydrogen-bonded network structure was suggested by Abdul-Sada et al. {88} for 1-alkyl-3-methylimidazolium halides based on results from fast-atom bombardment mass spectroscopy. Charge ordering in ILs was discussed by Hardacre et al. {53}. They obtained the radial distribution curves of dimethylimidazolium chloride and hexafluorophosphate liquids using neutron diffraction and argued for charge ordering of ions in ILs resembling what is found in the solid state. Charge ordering has also been discussed in a number of molecular dynamics computer simulation studies on 1-alkyl-3-methylimidazolium-based ILs in recent few years {7}, {84}, {85}, {89}, {90}, {91}, {92}, {93}, {94}, {95} {96}, {97}, {98}, {99}. The radial distribution functions calculated in these papers all have suggested long-range charge ordering, giving support to the idea that ILs are unique in having more structure ordering than do conventional molecular liquids.

Many unique properties may be expected to arise from these local structures in ILs. One example is the *unusually high viscosity* of certain ILs arising from the hindering of the translational motion of the ions. Magnetic behavior is another most unusual and interesting property that arise when magnetic ions (strongly interacting with one another) are locally aligned in a liquid. Recently it was demonstrated {100}, {101} that *magnetic* ILs can be made by mixing imidazolium chlorides ($[C_4C_1Im]Cl$ or $[nC_4C_1Im]Cl$) and $FeCl_3$, forming 1-butyl-3-methylimidazolium tetrachloroferrate $[C_4C_1Im][FeCl_4]$ and 1-butyronitrile-3-methylimidazolium tetrachloroferrate $[nC_4C_1Im][FeCl_4]$ (IUPAC name of $[nC_4C_1Im]^+$ cation: 1-(3-cyanopropyl)-3-methyl-1*H*-imidazol-3-ium). These nearly paramagnetic liquids show strong responses to magnetic fields, probably because of local ordering of the magnetic high-spin $[FeCl_4]^-$ anions. The surfaces of the liquids bend (deviate from being horizontal) when they are approached by a magnet, an interesting property that might find applications. FT-Raman spectroscopy indicated that the magnetic liquids contained $[C_4C_1Im]^+$ and $[nC_4C_1Im]^+$ cations. The constitution of the liquids thus were confirmed by their Raman spectra. By combining many different cations and

magnetic anions it might be possible to prepare superparamagnetic or even ferromagnetic ionic liquids {100}, {101}.

Another interesting behavior of an ionic liquid has been observed: The molecular arrangements of 1-butyronitrile-3-methylimidazolium halides, in the presence and absence of intruded water molecules, form a new kind of ice that has been studied by Raman spectroscopy {102}, {103}. Single crystals of the ice were isolated and the structure elucidated by single-crystal X-ray crystallography. Apparently the water changes the physical properties of the ionic liquid at the molecular level and this was found to change the conformation of the *n*-butyronitrile chain of the cation. The hydrogen bonding interaction between the anion and the water molecule seems to lead to loose molecular packing arrangements of the IL. As the unique properties are related to the structures and molecular arrangements of the ILs, the presence of water, wanted or unwanted, must be carefully examined in any kind of IL research and applications {103}.

X. Other systems

Raman spectra of N-butylpyridinium chloride - aluminum trichloride liquid systems (e.g. $[C_4py][AlCl_4]$, Fig. 1) were obtained at ambient temperatures already in 1978 {104}. The $[C_4py][FeCl_4]$ also is a IL, and in the phase diagram of the binary system $[C_4py]Cl$ - $FeCl_3$ liquids are formed in a wide mol fraction composition range from 0.26 to 0.58 {105}. Unrestricted HF calculations were performed with 6-31G* basis sets in order to predict the structures, energies, bond lengths, and vibrational (Raman) frequencies. Both the Raman scattering experiments and the *ab-initio* calculations indicate that $[FeCl_4]^-$ is the predominant anion in the ionic liquid at a mole fraction of 0.50 {105}.

The structure of the bis(trifluoromethylsulfonyl)imide ($[Tf_2N]^-$) anion in the liquid state has been investigated by means of IR and Raman spectroscopy and *ab-initio* self-consistent Hartree-Fock and DFT calculations on the free ion, aiming at a determination of the equilibrium geometry and understanding of the vibrational spectrum {80}, {89}, {90}, {106}, {107}, {108}. A pronounced

delocalization of the negative charge on the nitrogen and oxygen atoms was found, and a marked double-bond character of the S-N-S moiety for the anion {106}, {107}. A tentative assignment of some characteristic vibrations of the $[Tf_2N]^-$ anion was performed using the spectra of aqueous solutions for comparison in order to analyze the conformational isomerism and ion-pairing effects {106}{107}. Also it was found that dihedral S-N-S-C torsion angle in the bistriflylimide anion, has a complex energy profile which was precisely reproduced when tested by confrontation against liquid-phase Raman spectroscopic data {89}, {90}, {91}.

The Raman spectra of the $[C_2C_1Im][Tf_2N]$ show relatively strong bands arising from the $[Tf_2N]^-$ ion at ~398 and ~407 cm^{-1}, see Fig. 21 {108}. Interestingly, the ~407 cm^{-1} band, relative to the ~398 cm^{-1} one, grows appreciably in intensity with raising temperature. This feature is suggesting that an equilibrium is established between $[Tf_2N]^-$ conformers in the liquid state, see Fig. 22. According to the DFT calculations (followed by normal frequency analyses), two conformers (of C_2 or C_1 point group symmetry; two-fold rotational axis or no symmetry, respectively) constitute global and local minima, and have an energy difference of 2.2-3.3 kJ mol^{-1} {108}. The observed spectra over the range 380-440 cm^{-1} could be understood from the calculation of $[Tf_2N]^-$ conformers: The omega-SO_2 wagging vibration appeared at 396 and 430 cm^{-1} for the C_1 conformer and at 387 and 402 cm^{-1} for the C_2 one. The enthalpy of the conformational change from the most stable C_2 to C_1 came out in good agreement with the theoretical calculation. It was concluded that a conformational equilibrium indeed must exist between the C_1 and C_2 conformers of $[Tf_2N]^-$ in liquid $[C_2C_1Im][Tf_2N]$ {108}. Three different conformers (named *cis* and *trans* by the authors) have recently been found in the X-ray crystal structure of the salt $Li_2[C_2C_1Im][Tf_2N]_3$ {109}.

We were able to obtain the same wagging omega-SO_2 vibrational bands in our Raman spectrum of liqiud $[C_4C_1Im][Tf_2N]$, see Fig. 23. Apparently the splitting between the two bands (at 411 and 403 cm^{-1}) is not so large for the case of the 1-butyl-3-methylimidazolium bis(trifluoromethylsulfonyl)imide liquid. The symmetric CF_3 stretching and deformation bands are seen very strongly at ~1242 and ~742 cm^{-1} in our spectra, as found also by Rey et al. {106}, {107}. The bands at 500-750 cm^{-1} discussed in

relation with Fig. 7 can be faintly seen, showing that the AA/GA conformational equilibrium of the butyl group in $[C_4C_1Im]^+$ is established, as discovered by Hamaguchi et al. {50}.

The $[Tf_2N]^-$ anion was further studied and discussed in Raman investigations on the ionic liquid N-propyl-N-methylpyrrolidinium bis(trifluoromethylsulfonyl)imide ([P13][Tf_2N]) and its 2/1 mixture with Li[Tf_2N] {110}, as well as on the N-butyl-N-methylpyrrolidinium bis(trifluoromethanesulfonyl)imide ([P14][Tf_2N] or [4-C_1C_4py][Tf_2N]) and other useful reaction media such as [4-C_1C_4py][TfO] {111}, {112}. Raman results have also shown that $[Tf_2N]^-$ anions only interact weakly with $[P13]^+$ cations, but coordinated strongly to Li^+ cations over a temperature range extending from -100 to +60 °C, i.e. in the crystalline and melt states {113}.

By means of Raman spectroscopy and DFT calculations on the [4-C_1C_4py][Tf_2N] and [4-C_1C_4py]Br systems, various types of conformations with respect to the pyrrolidinium ring and N-butyl group were found {113}. The calculations indicated that, among others, the so-called *eq*- and ax-en*velope* conformers with the butyl group at equatorial and axial positions, respectively, against the plane of four atoms of the *envelope* pyrrolidinium ring (see Fig. 24) were relatively stable, and the former gave the global minimum {113}.

By comparing observed and calculated Raman spectra it was found that the $[4\text{-}C_1C_4py]^+$ ion was present mainly as the *ax-envelope* conformer in the [4-C_1C_4py]Br crystal, while the *eq*- and *ax-envelope* conformers were present in equilibrium in the [4-C_1C_4py][Tf_2N] ionic liquid (called [P14][TFSI] {113}). The presence of conformational equilibria was further experimentally supported by Raman spectra measured at different temperatures. It was established that the conformation of the butyl group was restricted to a so-called *trans-TT* conformation, in which the butyl group is located *trans* against a ring carbon atom (C2 or C5), and all carbon atoms in the butyl chain are located *trans* to each other {113}.

We have briefly investigated some $[4\text{-}C_1C_4py]^+$ room temperature liquids, namely $[4\text{-}C_1C_4py][Tf_2N]$ and $[4\text{-}C_1C_4py][TfO]$ {72}. he experimental Raman spectra of our liquids looked much like *sums* of the spectrum of the $[bmpy]^+$ ion (as measured from the chloride salt) and the spectra of the $[Tf_2N]^-$ or $[TfO]^-$ ions (as measured from the lithium salts). An example of our results on $[4\text{-}C_1C_4py][Tf_2N]$ is shown in Fig. 25. The spectra in Fig. 25 clearly show that the constituent ions in the liquid and in the respective solid salts vibrate *rather* independent of the surroundings. Therefore the liquid spectrum looks much like the sum of the solid salts. This conclusion is of course not new, but never the less it is still *quite* applicable in the evaluation of many IL Raman (and IR) spectra. However, the presence of conformational equilibria for both of the IL ions makes a closer study worth while. We therefore recommend the interested reader to study the work by Umebayashi et al. {113}, in which subtle spectral band shape details e.g. around 930-880 cm^{-1} are evaluated to show information on the *eq-envelope:trans-TT* and *ax-envelope:trans-TT* interconversion of the $[bC1Im]^+$ ion in the liquid. Also note that the crystal structure of the $[4\text{-}C_1C_4py][Tf_2N]$ salt was recently solved; it contained the *eq-envelope:trans-TT* conformer of the cation {114}. Also conformers of symmetry C_1 and C_2 of the $[Tf_2N]^-$ ion show their presence burried in the band at 400-440 cm^{-1} {108}.

Prior to the publication of the work by Umebayashi et al. {113} on the 1-butyl-1-methyl-pyrrolidinium bis(trifluoromethylsulfonyl)imide, some preliminary calculations were done aiming at a better understanding of the spectra on that system (shown in Fig. 25). To illustrate how useful such procedures are, we depict two examples of our own results in Fig. 26. The shown *ax-envelope:trans-TG* and *-TT* confomations are just some of the many possible conformations. The more likely ones, such as the *ax-envelope:trans-TT and eq-envelope:trans-TT* were included in the study by Umebayashi et al. {113}. The calculated spectra of the different conformers looked rather much like each other. As seen in Fig. 26 the *gauche* form of the C8-C9 bond did not change much relative to the *ax-envelope:trans-TT* form. Quite satisfactory one-to-one correspondences between calculated and observed bands are found in Fig. 26 and also in the work of Umebayashi et al. {113}. One should not expect perfect fits (frequencies are calculated too high and intensities are perturbed, because of the simplicity of the modelling).

When the theoretical spectra of the $[4\text{-}C_1C_4py]^+$ ion (e.g. those in Fig. 26) and similarly calculated spectra of conformations of the $[Tf_2N]^-$ ion (in Fig. 27, see later) were added, we obtained sums (not shown) that essentially corresponded to the spectrum of the $[4\text{-}C_1C_4py][Tf_2N]$ liquid (in Fig. 25, top) {72}.

New 2-hydroxypropyl-functionalized imidazolium cation ionic liquids (containing an appended hydroxyl functionality) have been made {115} by use of an "atom efficient one-pot reaction" between 1-methylimidazole and acid with propylene oxide. Unfortunately the systems were not studied by FT-Raman spectroscopy so far. We have shown in a study on 1-hexanol in [1,3-bis-[2-(methoxyethoxy)ethyl]imidazolium] bis-trifluoromethylsulfonyl-imide {29} that Raman spectroscopy has a potential for finding clues to what goes on in ionic liquids that contain hydroxyl groups (alkohols) and where hydrogen bonding between the ionic liquid and the hydroxyl group is of importance.

A rather new class of room temperature ionic liquids is based on the *N*,*N*,*N'*,*N'*-tetramethylguanidinium $[((CH_3)_2N)_2CNH_2]^+$ or $[TMGH]^+$ cation, see Fig. 1. A dedicated force field was developed {116} to fit the experimental bonds and angles and the vibration frequencies, for five kinds of $[TMGH]^+$ ILs, where the anion was formate, lactate, *per*chlorate, trifluoroacetate, and trifluoromethylsulfonate, respectively. *Ab-initio* calculations were performed and predictions in good agreement with the experimental data obtained. Radial and spatial distribution functions (RDFs and SDFs) were investigated to depict the microscopic structures of the ILs {13}.

An illustrative FT-Raman spectrum was recorded on the $[TMGH][Tf_2N]$ liquid to be compared with calculated spectra of the constituent isolated ions in their equlibrium geometries obtained at the RHF/6-31G(d) level using DFT/ B3LYP methods {49}. Some data obtained {72} are shown in Fig. 27. Unfortunately the highest-frequent N-H stretchings were out of our instrumental range (limited to 3500

– 100 cm^{-1}). However, many experimental details are being convincingly accounted for by the modelling, just by summation of the calculated spectra, even when other conformers are left out.

XI. Other Applications of Raman Spectroscopy

Raman spectroscopy has up to now mainly been applied to elucidate conformational forms and associated conformational equilibria of the ionic liquid components. Yet other applications are appearing in these years. One example is the characterization of metal ions like Mn^{2+}, Ni^{2+}, Cu^{2+} and Zn^{2+} in coordinating solvent mixtures by means of titration Raman Spectroscopy {117}. Another issue is the study of solvation of probe molecules in ionic liquids. In such a study {117}, e.g. acceptor numbers (AN) of ionic liquids in diphenylcyclopropenone (DPCP) were estimated by an empirical equation associated with a C=C / C=O stretching mode Raman band of DPCP. According to the dependence of AN on cation and anion species, the Lewis acidity of ionic liquids was considered to come mainly from the cation charge {118}.
Finally Raman spectroscopy has a potential of being used for qualitative and quantitative analysis. We have used Raman spectroscopy to verify the presence of components in a two-phase system {29}.

XII. Conclusions

Recently Raman spectroscopy has been applied - in combination with other methods - to show that certain characteristic spectral bands can be identified that are characteristic for conformational forms (conformers) of the ionic liquid components, and that the associated conformational equilibria might be partly responsible for the salts to have such low melting points.

In this review we have discussed in detail some examples of the conformational equilibria, e.g. those discovered by Hamaguchi, *et al.* {70} in liquids containing the 1-butyl-3-methylimidazolium cation. Also, we have examined in some detail liquids containing the bis(trifluoromethanesulfonyl)imide anion, as described above. We have extended the knowledge on the characteristic Raman bands to include conformers of the 1-hexyl-3-methylimidazolium cation {46}. Vibrational analysis has been

made of the components of the systems to improve our understanding of what goes on in the liquids. These results, although not surprising, add weight to our understanding of the existence of mixtures of low symmetry conformers that disturb the crystallisation process. Arguments have been presented for the belief that this is the reason for the low melting points of the ILs relative to "normal molecular salts" with much higer melting points.

We have seen that the *ab-initio* self-consistent quantum mechanical functional methods such as e.g. DFT/B3LYP with the chosen 6-31+G(d,p) basis sets are well suited to calculate reasonable molecular ion structures and vibrational spectra of these ions. The results obtained by us or others have indicated that the neglect of the prescence of cation-anion interactions is a reasonable approximation for a rather successful prediction of the Raman spectra. Based on such calculations detailed and relyable assignments of the spectra can be given and informtion on conformational equilibria obtained.

XIII. Acknowledgements

I would like to thank Niels J. Bjerrum, Anders Riisager, Rasmus Fehrmann and Irene Shim from Department of Chemistry, DTU, Denmark, Cory C. Pye from Department of Chemistry, Saint Mary's University, Halifax, Nova Scotia, Canada, N. Llewellyn Lancaster from Department of Chemistry, King's College, London University, UK, Ken Seddon, QUILL Research Centre, Queen's University Belfast, Northern Ireland, Mihkel Koel from Department of Chemistry, Tallin University of Technology, Estonia, and Susanne Brunsgaard Hansen (formerly from Department of Chemistry, DTU) for help with finishing the manuscript. Lykke Ryelund and Ole Faurskov Nielsen of the Department of Chemistry, H.C. Ørsted Institute, University of Copenhagen are thanked for much measurement assistance. The work was supported by the Technical University of Denmark.

XIV. References

{1} Wilkes, J.S., Properties of ionic liquid solvents for catalysis, J. Mol. Catal. A: Chem., 214, 11-17, 2004.

{2} Tait, S. and Osteryoung, R. A., Infrared study of ambient-temperature chloroaluminates as a function of melt acidity, Inorg. Chem., 23, 4352-4360, 1984.

{3} Dymek Jr., C. J. and Stewart, J. J. P., Calculation of hydrogen-bonding interactions between ions in room-temperature molten salts, Inorg. Chem., 28, 1472-1476, 1989.

{4} Hanke, C. G., Price, S. L. and Lynden-Bell, R. M., Intermolecular potentials for simulations of liquid imidazolium salts, Molec. Phys., 99, 801-809, 2001.

{5} Meng, Z., Dölle, A., and Carper, W. R, Gas phase model of an ionic liquid: semi-empirical and ab initio bonding and molecular structure, J. Molec. Struct. (THEOCHEM) 585, 119-128, 2002.

{6} Carper, W. R., Meng, Z., Wasserscheid, P. and Dölle, A., NMR relaxation studies and molecular modeling of 1-butyl-3-methylimidazolium PF_6, [BMIM][PF_6], International Symposium on Molten Salts, (P. C. Trulove, H. C. DeLong, and R. A. Mantz, eds.), Electrochem. Soc. Proceedings 2002-19 (Molten Salts XIII), 973-982, 2002.

{7} Shah, J. K., Brennecke, J. F. and Maginn, E. J., Thermodynamic properties of the ionic liquid 1-n-butyl-3 methylimidazolium hexafluorophosphate from Monte Carlo simulations, Green Chem. 4, 112-118, 2004.

{8} Dymek, C. J., Grossie, D. A,, Fratini, A. V. and Adams, W, W., Evidence for the presence of hydrogen bonded ion-ion interaction in the molten salt precursor, 1-methyl-3-ethylimidazolium chloride, J. Molec. Struct., 213, 25-34, 1989.

{9} Wilkes, J. S. and Zaworotko, M. J., Manifestations of noncovalent interactions in the solid state. Dimeric and polymeric self-assembly in imidazolium salts via face-to-face cation-cation Π-stacking, Supramolec. Chem. 1, 191-193, 1993.

{10} Fuller, J., Carlin, R.T., DeLong, H.C. and Haworth, D., Structure of 1-ethyl-3-methylimidazolium hexafluorophosphate: Model for room temperature molten salts, Chem. Commun., 299-300, 1994.

{11} Carmichael, A. J., Hardacre, C., Holbrey, J. D., Nieuwenhuyzen, M. and Seddon, K. R., Molecular layering and local order in thin films of 1-alkyl-3-methylimidazolium ionic liquids using X-ray reflectivity, Molec. Phys., 99, 795-800, 2001.

{12} Bradley, A. E., Hardacre, C., Holbrey, J. D., Johnston, S., McMath, S, E, J. and Nieuwenhuyzen, M., Small-Angle X-ray Scattering Studies of Liquid Crystalline 1-Alkyl-3-methylimidazolium Salts, Chem. Mater., 14, 629-635, 2002.

{13} Huang, J., Riisager, A., Wasserscheid, P. and Fehrmann, R., Reversible physical absorption of SO_2 by ionic liquids, Chem. Commun., 2006, 4027-4029, 2006.

{14} Huang, J., Riisager, A., Berg, R. W. and Fehrmann, R., Tuning Ionic Liquids for High Gas Solubility and Reversible Gas Sorption, J. Mol. Catalysis A (Chemical), Elsevier, Doi: 10.1016/j.molcala.2007.07.036, in print 2007.

{15} Elaiwi, A., Hitchcock, P. B., Seddon, K. R., Srinivasan, N., Tan, Y. M., Welton, T. and Zora, J. A., Hydrogen bonding in imidazolium salts and its implications for ambient-temperature

halogenoaluminate(III) ionic liquids, J. Chem. Soc., Dalton Trans. 1995, 3467-3472, 1995.

{16} Katsyuba, S. A., Dyson, P. J., Vandyukova, E. E., Chernova, A. V. and Vidis, A., Molecular structure, vibrational spectra, and hydrogen bonding of the ionic liquid 1-ethyl-3-methyl-1H-imidazolium tetrafluoroborate. Helv. Chim. Acta, 87, 2556-2565, 2004.

{17} Cammarata, L., Kazarian, S.G., Salter, P.A. and Welton, T., Molecular states of water in room temperature ionic liquids, Phys. Chem. Chem. Phys., 3, 5192-5200, 2001.

{18} Storhaug, V.J. and Carper, W.R., AB initio molecular structure and vibrational spectra of ionic liquids. Trends in Physical Chemistry, 9, 173-177, 2003.

{19} Endres, F. and Zein El Abedin, S., Air and water stable ionic liquids in physical chemistry, Phys. Chem. Chem. Phys., 8, 2101-2116, 2006.

{20} Gilbert, B., Chauvin, Y. and Guibard, I., Investigation by Raman Spectrometry of a New Room-temperature organochloroaluminate molten salt, Vib. Spectrosc., 1, 299-304, 1991.

{21} Gilbert, B., Pauly, J.P., Chauvin, Y. and Di Marco-Van Tiggelen, F., Raman Spectroscopy of Room Temperature Organochloroaluminate Molten Salts, Proc. 9th Int. Symposium on Molten Salts, C. L. Hussey et al., Eds., Electrochem. Soc., Pennington, NJ., Vol. 94-13, 218-226, 1994.

{22} Chauvin, Y., Di Marco-Van Tiggelen, F. and Olivier, H., Determination of aluminuium electronegativity in new ambient-temperature acidic molten salts, J. Chem. Soc., Dalton Trans., 1009-1011, 1993.

{23} Howlett, P. C., Brack, N., Hollenkamp, A. F., Forsyth, M., and MacFarlane, D. R., Characterization of the Lithium Surface in N-Methyl-N-alkylpyrrolidinium

Bis(trifluoromethanesulfonyl)imide Room - Temperature Ionic Liquid Electrolytes, J. Electrochem. Soc., 153, A595-A606, 2006.

{24} He Ping, Liu Hongtao, Li Zhiying, Liu Yang, Xu Xiudong, Li Jinghong, Electrochemical deposition of silver in room - temperature ionic liquids and its surface-enhanced Raman scattering effect, Langmuir, 20, 10260-10267, 2004.

{25} Schafer, T., Di Paolo, R. E., Franco R. and Crespo, J. G., Elucidating interactions of ionic liquids with polymer films using confocal Raman spectroscopy, Chem. Commun., 20, 2594-2596, 2005.

{26} Nanbu, N., Sasaki, Y. and Kitamura, F., In situ FT-IR spectroscopic observation of a room-temperature molten salt gold electrode interphase, Electrochem. Commun., 5, 383-387, 2003.

{27} Santos, V. O. Jr., Alves, M. B., Carvalho, M. S., Suarez, P. A. Z. and Rubim, J. C., Surface-enhanced Raman scattering at the silver electrode/ ionic liquid ($BMIPF_6$) interface, J. Phys. Chem. B, 110, 20379-20385, 2006.

{28} Romero, C. and Baldelli, S., Sum frequency generation study of the room - temperature ionic liquids /quartz interface, J. Phys. Chem. B, 110, 6213-6223, 2006.

{29} Riisager, A., Fehrmann, R., Berg, R. W., van Hal, R. and Wasserscheid, P., Thermomorphic phase separation in ionic liquid-organic liquid systems-conductivity and spectroscopic characterization, Phys. Chem. Chem. Phys., 7, 3052-3058, 2005.

{30} Raman, C. V. and Krishnan, K. S., A new Type of Secondary Radiation, Nature, 121, 501, 1928.

{31} Herzberg, G. Molecular Spectra and Molecular Structure, Vol. II, Infrared and Raman Spectra of Polyatomic Molecules, van Nostrand, New York, 1945.

{32} Wilson, E.B.Jr., Decius, J.C. and Cross, P.C., Molecular Vibrations, The Theory of Infrared and Raman Vibrational Spectra, McGraw-Hill Book Co., New York, 1955.

{33} Long, D. A., The Raman Effect: A Unified Treatment of the Theory of Raman Scattering by Molecules, John Wiley and Sons, ISBN 0471490288, 2002.

{34} Diem, M., Introduction to Modern Vibrational Spectroscopy, J. Wiley & Sons, New York, USA, 1993.

{35} Laserna, J. J. (Ed.), Modern Techniques in Raman Spectroscopy, J. Wiley & Sons, Chichester UK, 1996.

{36} Coates, J., Vibrational spectroscopy: instrumentation for infrared and Raman spectroscopy. Appl. Spectrosc. Rev. 33, 267-425, 1998.

{37} McCreery, R. L., Raman Spectroscopy for Chemical Analysis, J. Wiley & Sons, Chichester, 1-415, 2001.

{38} Smith, E. and Dent, G. Modern Raman Spectroscopy - A practical Approach, J. Wiley & Sons, Ltd., ISBN 0-471-49668-5, 1-210, 2005.

{39} Lin-Vien, D., Colthup, N. B., Fateley, W. G., Grasselli, J. G., Handbook of Infrared and Raman Characteristic Frequencies of Organic Molecules, Academic Press, New York, 1991.

{40} Nyquist, R. A., Kagel, R. O., Putzig, C. L, Leugers, M. A., Handbook of Infrared and Raman Spectra of Inorganic Compounds and Organic Salts (4 vols.), Academic Press, New York and London, 1996.

{41} Nakamoto, K., Infrared and Raman Spectra of Inorganic and Coordination Compounds, 5th ed., Part A: Theory and Applications in Inorganic Chemistry, and Part B, Applications in Coordination, Organometallic and Bioinorganic Chemistry, John Wiley & Sons, New York, 1997.

{42} Socrates, G, Infrared and Raman Characteristic Group Frequencies, Tables and Charts, 3rd ed., J. Wiley & Sons, Chichester UK, 1-249, 2001.

{43} Carter, R. L. Molecular Symmetry and Group Theory, John Wiley & Sons, New York, 1998.

{44} Atkins, P. W. and Friedman, R. S, Molecular Quantum Mechanics, 4th edition, Oxford University Press, ISBN: 13978-0-19-927498-7, 1-608, 2004.

{45} Chase, D.B., and Rabolt, J. F., Fourier Transform Raman Spectroscopy, Academic Press, New York, 1994.

{46} Berg, R. W., Deetlefs, M., Seddon, K. R., Shim, I. and Thompson, J. M., Raman and ab initio studies of simple and binary 1-alkyl-3-methylimidazolium ionic liquids, J. Phys. Chem. B, 109, 19018-19025, 2005. See also supplementary information at http://pubs.acs.org/subscribe/journals/jpcbfk/suppinfo/jp050691r/jp050691rsi20050208_105000.pdf .

{47} Atkins, P. and de Paula, J., Atkins' Physical Chemistry, 8th Edition, Oxford University Press, 2006.

{48} Ratner, M. A. and Schatz, G. C., Introduction to Quantum Mechanics in Chemistry, Prentice-Hall Inc. N.J., ISBN 0-13-895491-7, 305 p., 2001.

{49} Frisch, M. J., Trucks, G. W., Schlegel, H. B., Scuseria, G. E., Robb, M. A., Cheeseman, J. R.,

Montgomery, J. A. Jr., Vreven, T., Kudin, K. N., Burant, J. C., Millam, J. M., Iyengar, S. S., Tomasi, J., Barone, V., Mennucci, B., Cossi, M., Scalmani, G., Rega, N., Petersson, G. A., Nakatsuji, H., Hada, M., Ehara, M., Toyota, K., Fukuda, R., Hasegawa, J., Ishida, M., Nakajima, T., Honda, Y., Kitao, O., Nakai, H., Klene, M., Li, X., Knox, J. E., Hratchian, H. P., Cross, J. B., Adamo, C., Jaramillo, J., Gomperts, R., Stratmann, R. E., Yazyev, O., Austin, A. J., Cammi, R., Pomelli, C., Ochterski, J. W., Ayala, P. Y., Morokuma, K., Voth, G. A., Salvador, P., Dannenberg, J. J., Zakrzewski, V. G., Dapprich, S., Daniels, A. D., Strain, M. C., Farkas, O., Malick, D. K., Rabuck, A. D., Raghavachari, K., Foresman, J. B., Ortiz, J. V., Cui, Q., Baboul, A. G., Clifford, S., Cioslowski, J., Stefanov, B. B., Liu, G., Liashenko, A., Piskorz, P., Komaromi, I., Martin, R. L., Fox, D. J., Keith, T., Al-Laham, M. A., Peng, C. Y., Nanayakkara, A., Challacombe, M., Gill, P. M. W., Johnson, B., Chen, W., Wong, M. W., Gonzalez, C., and Pople, J. A., Gaussian 03, Revision C.02, Gaussian, Inc.: Wallingford CT, 2004.

{50} Hamaguchi, H. and Ozawa, R., Structure of ionic liquids and ionic liquid compounds: Are ionic liquids genuine liquids in the conventional sense?, Adv. Chem. Phys., 131, 85-104, 2005.

{51} Gordon, C. M., Holbrey, J. D., Kennedy, A. R., Seddon, K. R., Ionic Liquid Crystals: hexafluorophosphate salts, J. Mater. Chem., 8, 2627-2636, 1998.

{52} Holbrey, J. D. and Seddon, K. R., The phase behaviour of 1-alkyl-3-methylimidazolium tetrafluoroborates; ionic liquids and ionic liquid crystals, J. Chem. Soc., Dalton Trans., 2133-2139, 1999.

{53} Triolo, A., Mandanici, A., Russina, O., Rodriguez-Mora, V., Cutroni, M., Hardacre, C., Nieuwenhuyzen, M., Bleif, H.-J., Keller, L., Ramos, M. A., Thermodynamics, Structure, and Dynamics in Room Temperature Ionic Liquids: The Case of 1-Butyl-3-methyl Imidazolium Hexafluorophosphate ([bmim][PF_6]), J. Phys. Chem. B 110, 21357-21364, 2006.

{54} Triolo, A., Russina, O., Arrighi, V., Juranyi, F., Janssen, S., Gordon, C. M., Quasielastic neutron scattering characterization of the relaxation processes in a room temperature ionic liquid, J. Chem. Phys. 119, 8549-8557, 2003.

{55} Roche, J. D., Gordon, C. M., Imrie, C. T., Ingram, M. D., Kennedy, A. R., Lo Celso, F. and Triolo, A., Application of Complementary Experimental Techniques to Characterization of the Phase Behavior of $[C_{16}mim][PF_6]$ and $[C_{14}mim][PF_6]$, Chem. Mater., 15, 3089-3097, 2003.

{56} Firestone, M. A., Dzielawa, J. A., Zapol, P., Curtiss, L. A., Seifert, S. and Dietz, M. L., Lyotropic Liquid-Crystalline Gel Formation in a Room-Temperature Ionic Liquid, Langmuir, 18, 7258-7260, 2002.

{57} Saha, S., Hayashi, S., Kobayashi, A. and Hamaguchi, H., Crystal structure of 1-butyl-3-methylimidazolium chloride. A clue to the elucidation of the ionic liquid structure, Chemistry Letters (Japan) 32, 740-741, 2003.

{58} Holbrey, J. D., Reichert, W. M., Nieuwenhuyzen, M., Johnston, S., Seddon, K. R., Rogers, R. D., Crystal polymorphism in 1-butyl-3-methylimidazolium halides: supporting ionic liquid formation by inhibition of crystallization, Chem. Commun., 1636-1637, 2003.

{59} Katayanagi, H., Hayashi, S., Hamaguchi, H., Nishikawa, K., Structure of an ionic liquid, 1-n-butyl-3-methylimidazolium iodide, studied by wide-angle X-Ray scattering and Raman Spectroscopy, Chem. Phys Lett., 392, 460-464, 2004.

{60} Bowers, J., Vergara-Gutierrez, M. C. and Webster, J. R. P., Surface Ordering of Amphiphilic Ionic Liquids, Langmuir, 20, 309-312, 2004.

{61} Bowers, J., Butts, C. P., Martin, P. J., Vergara-Gutierrez, M. C. and Heenan, R. K., Aggregation

Behavior of Aqueous Solutions of Ionic Liquids, Langmuir, 20, 2191-2198, 2004.

{62} Takahashi, S., Curtiss, L.A., Gosztola, D., Koura, N. and Saboungi, M.- L., Molecular Orbital Calculations and Raman Measurements for 1-ethyl-3-methylimidazolium chloroaluminates, Inorg. Chem., 34, 2990-2993, 1995.

{63} J. G. Huddleston, A. E. Visser, W. M. Reichert, H. D. Willauer, G. A. Broker, and R. D. Rogers, Characterization and comparison of hydrophilic and hydrophobic room temperature ionic liquids incorporating the imidazolium cation, Green Chem. 3, 156-164, 2001.

{64} Hayashi, S., Ozawa, R., Hamaguchi, H., Raman spectra, crystal polymorphism, and structure of a prototype ionic-liquid [bmim]Cl, Chem. Lett., 32, 498-499, 2003.

{65} Nishikawa, K., Wang, S., Katayanagi, H., Hayashi, S., Hamaguchi, H., Koga, Y. and Tozaki, K., Melting and Freezing Behaviors of Prototype Ionic Liquids, 1-Butyl-3-methylimidazolium Bromide and Its Chloride, Studied by Using a Nano-Watt Differential Scanning Calorimeter, J. Phys. Chem. B, 111, 4894-4900, 2007.

{66} Cambridge Crystallographic Data Centre, [C4mim]Cl "Crystal (1)" and [C4mim]Br data are registered as CCDC deposition number 213959 and 213960, respectively, see http://www.ccdc.cam.ac.uk.

{67} Aakeröy, C. B., Evans, T. A., Seddon, K. R., Pálinkó, I., The C-H...Cl hydrogen bond: does it exist?, New Journal of Chem., 23, 145-152, 1999.

{68} van den Berg, J.-A., Seddon, K. R., Critical Evaluation of C-H... X Hydrogen Bonding in the Crystalline State, Crystal Growth & Design 3, 643-661, 2003.

{69} Matsumoto, K., Hagiwara, R., Mazej, Z., Benkiˇc, P. and Žemva, B., Crystal structures of frozen room temperature ionic liquids, 1-ethyl-3-methylimidazolium tetrafluoroborate ($EMImBF_4$), hexafluoroniobate ($EMImNbF_6$) and hexafluorotantalate ($EMImTaF_6$), determined by low-temperature X-ray diffraction, Solid State Sciences 8, 1250–1257, 2006.

{70} Ozawa, R., Hayashi, S., Saha, S., Kobayashi, A. and Hamaguchi, H., Rotational isomerism and structure of the 1-butyl-3-methylimidazolium cation in the ionic liquid state, Chem. Lett. 32, 948-949, 2003.

{71} Okajima, H., Hamaguchi, H., Low frequency Raman Spectroscopy and liquid structure of imidazolium based ionic liquids. Abstracts of Papers, 231st ACS National Meeting, Atlanta, GA, United States, March 26-30, 2006, IEC-015. Publisher: American Chemical Society, Washington, D. C, 2006.

{72} Berg, R. W., unpublished results, 2006.

{73} Turner, E. A., Pye, C. C. and Singer, R. D., Use of ab Initio Calculations toward the Rational Design of Room Temperature Ionic Liquids, J. Phys. Chem. A, 107, 2277-2288, 2003.

{74} Talaty, E.R., Raja, S., Storhaug, V.J., Dölle, A., Carper, W.R., Raman and Infrared Spectra and ab Initio Calculations of $C_{2\text{-}4}$MIM Imidazolium Hexafluorophosphate Ionic Liquids, J. Phys. Chem. B, 108, 13177-13184, 2004.

{75} Antony, J. H., Mertens, D., Dölle, A., Wasserscheid, P., and Carper, W. R. Molecular reorientational dynamics of the neat ionic liquid 1-butyl-3-methylimidazolium hexafluorophosphate by measurement of ^{13}C nuclear magnetic relaxation data., Chem. Phys. Chem., 4, 588-594, 2003.

{76} Antony, J.H., Mertens, D., Breitenstein, T., Dölle, A., Wasserscheid, P. and Carper, W. R., Molecular structure, reorientational dynamics, and intermolecular interactions in the neat ionic liquid 1-butyl-3-methylimidazolium hexafluorophosphate, Pure and Appl. Chem. 76, 255-261, 2004.

{77} Heimer, N.E., Del Sesto, R.E. and Carper, W.R., Evidence for spin diffusion in a H,H-NOESY study of imidazolium tetrafluoroborate ionic liquids, Magn. Reson. Chem., 42, 71-75, 2004.

{78} Heimer, N.E., Del Sesto, R.E., Meng, Z., Wilkes, J.S., and Carper, W.R., Vibrational spectra of imidazolium tetrafluoroborate ionic liquids, J. Mol. Liquids, 124, 84-95, 2006.

{79} Matsumoto, K., Hagiwara, R., Yoshida, R., Ito, Y., Mazej, Z., Benkic, P., Zemva, B., Tamada, O., Yoshino, H. and Matsubara, S., Syntheses, structures and properties of 1-ethyl-3-methylimidazolium salts of fluorocomplex anions, Dalton Transactions, 144-149, 2004.

{80} Umebayashi, Y., Fujimori, T, Sukizaki, T., Asada, M., Fujii, K., Kanzaki, R., Ishiguro, S.-i., Evidence of Conformational Equilibrium of 1-Ethyl-3-methylimidazolium in Its Ionic Liquid Salts: Raman Spectroscopic Study and Quantum Chemical Calculations, J. Phys. Chem. A, 109, 8976-8982, 2005.

{81} Downard, A., Earle, M. J., Hardacre, C., McMath, S. E. J., Nieuwenhuyzen, M. and Teat, S. J., Structural Studies of Crystalline 1-Alkyl-3-Methylimidazolium Chloride Salts, Chem. Mater., 16, 43-48, 2004.

{82} Giraud, G., Gordon, C. M., Dunkin, I. R. and Wynne, K., The effects of anion and cation substitution on the ultrafast solvent dynamics of ionic liquids: A time-resolved optical Kerr-effect spectroscopic study. J. Chem. Phys. 119, 464-477, 2003.

{83} Shigeto, S. and Hamaguchi, H., Evidence for mesoscopic local structures in ionic liquids: CARS signal spatial distribution of $C_n$mim[PF_6] (n = 4, 6, 8), Chem. Phys. Letters, 427, 329-332, 2006.

{84} Morrow, T. I. and Maginn, E. J., Molecular Dynamics Study of the Ionic Liquid 1-n-Butyl-3-methylimidazolium Hexafluorophosphate, J. Phys. Chem. B 106, 12807-12813 (2002), and Morrow, T. I. and Maginn, E. J., Erratum to document, J. Phys. Chem. B, 107, 9160, 2003.

{85} Shah J. K. and Maginn, E. J., A Monte Carlo simulation study of the ionic liquid 1-n-butyl-3-methylimidazolium hexafluorophosphate: liquid structure, volumetric properties and infinite dilution solution thermodynamics of CO_2, Fluid Phase Equilibria, 222-223, 195-203,2004.

{86} Hamaguchi, H., Saha, S., Ozawa, R., Hayashi, S., Raman and X-ray studies on the structure of [bmim]X (X = Cl, Br, I, [BF_4], [PF_6]): rotational isomerism of the $[bmim]^+$ cation, ACS Symposium Series 901 (Ionic Liquids IIIA: Fundamentals, Progress, Challenges, and Opportunities), 68-78, 2005.

{87} Canongia Lopes, J. N., Costa Gomes, M. F., Pádua, A. A. H., Nonpolar, polar, and associating solutes in ionic liquids, J. Phys. Chem. B 110, 16816-16818, 2006.

{88} Abdul-Sada, A. K., Elaiwi, A. E., Greenway, A. M., Seddon, K. R., Evidence for the clustering of substituted imidazolium salts via hydrogen bonding under the conditions of fast atom bombardment mass spectrometry, Eur. Mass Spectrom., 3, 245-247, 1997.

{89} Canongia Lopes, J.N., Deschamps, J., and Pádua, A.A.H., Modeling Ionic Liquids Using a Systematic All-Atom Force Field, J. Phys. Chem. B. 108, 2038-2047 and correction 11250, 2004.

{90} Canongia Lopes, J.N. and Pádua, A.A.H., Molecular Force Field for Ionic Liquids Composed of Triflate or Bistriflylimid Anions, J. Phys. Chem. B 108, 16893-16898, 2004.

{91} Canongia Lopes, J. N. A. and Pádua, A. A. H., Using Spectroscopic Data on Imidazolium Cation Conformations To Test a Molecular Force Field for Ionic Liquids, J. Phys. Chem. B, 110, 7485-7489, 2006.

{92} Canongia Lopes, J. N. A. and Pádua, A. A. H., Nanostructural Organization in Ionic Liquids, J. Phys. Chem. B 110, 3330-3335, 2006.

{93} De Andrade, J., Böes, E. S. and Stassen, H., A force field for liquid state simulations on room temperature molten salts: 1-ethyl-3methylimidazolium tetrachloroaluminate, J. Phys. Chem., B106, 3546-3548, 2002.

{94} De Andrade, J., Boes, E. S. and Stassen, H., Computational study of room temperature molten salts composed by 1-alkyl-3methylimidazolium cations - force field proposal and validation, J. Phys. Chem., B106, 13344-13351, 2002.

{95} Margulis, C. J., Stern, H. A. and Berne, B. J., Computer simulation of a "green chemistry" room-temperature ionic solvent, J. Phys. Chem. B 106, 12017-12021, 2002.

{96} Del Pópolo, M. G. and Voth, G. A., On the structure and dynamics of ionic liquids, J. Phys. Chem. B 108, 1744-1752, 2004.

{97} Yan, T., Burnham, C. J., Del Pópolo, M. G. and Voth, G. A., Molecular dynamics simulation of ionic liquids: The effect of electronic polarizability, J. Phys. Chem. B 108, 11877-11881, 2004.

{98} Liu, Z., Huang, S. and Wang, W., A refined force field for molecular simulation of imidazolium-based ionic liquids, J. Phys. Chem. B 108, 12978-12989, 2004.

{99} Urahata, S. M. and Ribeiro, M. C. C., Structure of ionic liquids of 1-alkyl-3-methylimidazolium cations: A systematic computer simulation study, J. Chem. Phys. 120, 1855-1863 (2004).

{100} Hayashi, S. and Hamaguchi, H., Discovery of a magnetic ionic liquid [bmim]$FeCl_4$, Chem. Lett., 33, 1590-1591, 2004.

{101} Hayashi, S., Saha, S., and Hamaguchi, H., A new class of magnetic fluids: bmim[$FeCl_4$] and nbmim[$FeCl_4$] ionic liquids, IEEE Transactions on Magnetics 42, 12-14, 2006.

{102} Miki, H., Hayashi, S., Kikura, H., and Hamaguchi, H., Raman spectra indicative of unusual water structure in crystals formed from a room-temperature ionic liquid, J. Raman Spectros., 37, 1242-1243, 2006.

{103} Saha, S. and Hamaguchi, H., Effect of water on the molecular structure and arrangement of nitrile-functionalized ionic liquids. J. Phys. Chem. B 110, 2777-2781, 2006.

{104} Gale, R. J., Gilbert, B., and Osteryoung, R. A., Raman spectra of molten aluminum chloride: 1-butylpyridinium chloride systems at ambient temperatures, Inorg. Chem., 17, 2728-2729, 1978.

{105} Tian, P., Song, X., Li, Y., Duan, J., Liang, Z. and Zhang, H., Studies on room temperature ionic liquid $FeCl_3$ - n-butylpyridinium chloride (BPC) system. Huaxue Xuebao, 64(23), 2305-2309, 2006. Journal written in Chinese, cited from Chemical Abstracts.

{106} Rey, I., Johansson, P., Lindgren, J., Lassegues, J. C, Grondin, J. and Servant, L. , Spectroscopic and Theoretical Study of $(CF_3SO_2)_2N^-$ ($TFSI^-$) and $(CF_3SO_2)_2NH$ (HTFSI), J. Phys. Chem. A, 102, 3249-3258, 1998.

{107} Rey, I., Lassegues, J. C., Grondin, J. and Servant, L., Infrared and Raman study of the PEO-LiTFSI polymer electrolyte, Electrochim. Acta, 43, 1505-1510, 1998.

{108} Fujii, K., Fujimori, T., Takamuku, T., Kanzaki, R., Umebayashi, Y. and Ishiguro, S., Conformational Equilibrium of Bis(trifluoromethanesulfonyl) Imide Anion of a Room - Temperature Ionic Liquid: Raman Spectroscopic Study and DFT Calculations, J. Phys. Chem.B 110, 8179-8183, 2006.

{109} Matsumoto, K., Hagiwara, R. and Tamada, O., Coordination environment around the lithium cation in solid $Li_2(EMIm)(N(SO_2CF_3)_2)_3$ (EMIm = 1-ethyl-3-methylimidazolium): Structural clue of ionic liquid electrolytes for lithium batteries, Solid State Sciences 8, 1103–1107, 2006.

{110} Castriota, M., Caruso, T., Agostino, R. G., Cazzanelli, E., Henderson, W.A. and Passerini, S., Raman Investigation of the Ionic Liquid N-Methyl-N-propylpyrrolidinium Bis(trifluoromethanesulfonyl)imide and Its Mixture with $LiN(SO_2CF_3)_2$, J. Phys. Chem. A, 109, 92-96, 2005.

{111} Lancaster, N. L., Salter, P. A., Welton, T. and Young, G. Brent, Nucleophilicity in ionic liquids. 2. Cation effects on halide nucleophilicity in a series of bis[tri-fluoromethylsulfonyl]imide ionic liquids, J. Org. Chem., 67, 8855-8861, 2002.

{112} Dal, E. and Lancaster, N. L., Acetyl nitrate nitrations in [bmpy][$N(Tf)_2$] and [bmpy][OTf], and the recycling of ionic liquids, Org. Biomol. Chem., 3, 682-686, 2005.

{113} Fujimori, T., Fujii, K., Kanzaki, R., Chiba, K. Yamamoto, H., Umebayashi, Y. and Ishiguro, S.-i., Conformational structure of room temperature ionic liquid N-butyl-N-methyl-pyrrolidinium bis(trifluoromethanesulfonyl)imide - Raman spectroscopic study and DFT calculations, J. Mol. Liquids 131-132 (Complete), 216-224, 2007.

{114} Choudhury, A. R., Winterton, N, Steiner, A., Cooper, A. I. and Johnson, K. A., In situ Crystallization of Low-Melting Ionic Liquids, J. Am. Chem. Soc., 127, 16792-16793, 2005.

{115} Holbrey, J.D., Turner M.B., Reichert, W.M. and Rogers, D.R., New ionic liquids containing an appended hydroxyl functionality from the atomefficient, one-pot reaction of 1-methylimidazole and acid with propylene oxide, Green Chem., 5, 731-736, 2003.

{116} Liu, X., Zhang, S., Zhou, G., Wu, G., Yuan, X. and Yao, X., New Force Field for Molecular Simulation of Guanidinium-Based Ionic Liquids, J. Phys. Chem. B, 110, 12062-12071, 2006.

{117} Ishiguro, S.-I., Umebayashi, Y. and Kanzaki, R., Characterization of Metal Ions in Coordinating Solvent Mixtures by Means of Raman Spectroscopy, Anal. Sci. (Japan), 20, 415-421, 2004.

{118} Fujisawa, T., Fukuda, M., Terazima, M. and Kimura, Y., Raman Spectroscopy Study on Solvation of Diphenylcyclopropenone and Phenol Blue in Room Temperature Ionic Liquids, J. Phys. Chem. A, 110, 6164-6172, 2006.

Table 1. Approximate descriptions* of vibrational frequencies (IR and Raman bands) as determined in MP2 calculations for the $[C_4C_1Im]^+$ cation with the butyl group either in the AA (*anti-anti*) conformation or in the GA (*gauche-anti*) conformation, derived from movements as depicted on a PC-screen.

	butyl group in the ***AA*** (*anti-anti*) conformation		butyl group in the ***GA*** (*gauche-anti*) conformation	
Mode	ν/cm^{-1}	Approximate Description	ν/cm^{-1}	Approximate Description
1	30.4	N-C7 tor	27.5	N-C7 tor
2	58.3	N-C6 tor	58.3	N-C6 tor
3	74.3	C7-C8 tor	76.6	N-C6 tor + C7-C8 tor
4	81.8	N-C6 tor + N-C7-C8 bend	82.5	C7-C8 tor
5	116.5	N-C7 tor	156.7	N-C6 oopl bend + $C8H_2$ rock
6	203.6	chain def + N-C6 oopl bend	205.1	chain def + N-C6 oopl bend
7	250.9	N-C6 + N-$C7H_2$ oopl ooph bend	251.1	N-C6 + N-$C7H_2$ oopl ooph bend
8	252.8	C9-C10 tor	258.4	C9-C10 tor
9	278.8	$C7H_2$ rock + $C6H_3$ ipl iph bend	296.1	$C7H_2$ rock + $C6H_3$ ipl iph bend
10	327.1	ring wag + chain def	333.3	ring wag + chain def
11	407.0	ring rot + $C7H_2$ rock + $C6H_3$ rock	418.0	ring rot + $C7H_2$ rock + N-$C6H_3$ ipl rock
12	441.0	N-C7 oopl bend + N-C6 oopl ooph bend + chain bend + CH_2 wag + ring rot	503.7	N-C7 oopl bend + N-C7-C8-C9 angles bend
13	619.6	ring oopl def + $C7H_2$ rock + C7-C8-C9 bend	603.9	N-C6 N-C7 iph str + ring oopl def + $C8H_2$ rock + N-C7-C8 bend.
14	636.2	ring def (C2-H oopl bend) + N-C6 N-C7 iph str + $C7H_2$ rock + C7-C8-C9 bend	622.8	ring def (C2-H C4-H iph oopl bend) + $C8H_2$ rock + N-C7-C8 bend.
15	670.2	N-C6 str + ring def (N1 and H on C2 oopl ooph departure) + $C8H_2$ wag + N-C7-C8 bend	662.8	ring def (bend around line NN) + $C8H_2$ rock + N-C7-C8 bend
16	725.5	Ring C-H oopl bend (bend around NN line)	712.8	N-C6 N-C7 ooph str + ring ipl def + $C8H_2$ rock + C7-C8 tor
17	748.8	N-C6 N-C7 ooph str + ring ipl def + N-C7-C8 and C7-C8-C9 bend	725.1	Ring C-H oopl bend (bend around NN line)
18	754.6	chain CH_2 sci + rock	773.5	Chain CH_2 rock + ring C-H oopl iph bend (umbrella)
19	791.7	ring C-H oopl iph bend (umbrella)	790.4	ring C-H oopl iph bend (umbrella)
20	813.7	C4-H C5-H oopl ooph bend (twi)	811.5	C4-H C5-H oopl ooph bend (twi)
21	819.3	chain CH_2 sci	853.9	Chain CH_2 sci
22	945.3	chain def + $C10H_2$ rock	912.4	Chain def + $C10H_3$ rock
23	969.8	chain def (CH_2 twi + rock)	981.5	Chain def (CH_2 sci + rock)
24	1043.6	ring def + chain def	1025.7	ring def + chain def
25	1057.3	ring def + N-C6 str + C4-H C5-H ipl iph bend	1051.9	ring def + N-C6 str + N-C7 str + C7-C8 str

26	1070.3	C4-H ipl bend + C7-C8 str	1064.0	C4-H C5-H ipl bend (sci) + N-C6 str + N-C7 str + C7-C8 str
27	1106.6	chain def	1104.9	Chain def
28	1128.4	$C6H_3$ ipl rock + ring def	1127.4	$C6H_3$ ipl rock + ring def
29	1149.9	C4-H C5-H ipl bend (sci)	1151.0	C4-H C5-H ipl bend (sci)
30	1167.0	chain def (C-C str)	1162.6	Chain def (C-C str)
31	1176.9	$C6H_3$ def (oopl rock)	1176.4	$C6H_3$ def (oopl rock)
32	1182.7	C2-H ipl bend, $C6H_3$ def, chain CH_2 def	1180.5	C2-H ipl bend, $C6H_3$ def, chain CH_2 def
33	1212.3	C6-N C7-N ooph str + ring C-H ipl bend	1211.1	C6-N C7-N ooph str + ring C-H ipl bend
34	1272.5	ring CH iph ipl bend + chain CH_2 def	1263.6	ring CH iph ipl bend + chain CH_2 def
35	1318.4	ring CH iph ipl bend + chain CH_2 wag	1311.0	ring CH iph ipl bend + chain CH_2 def
36	1324.3	ring CH iph ipl bend + chain CH_2 def	1329.2	ring CH iph ipl bend + chain CH_2 def
37	1353.0	chain CH_2 def + ring CH iph ipl bend	1362.5	Chain CH_2 def
38	1371.8	$C8H_2$ $C9H_2$ twi	1371.7	Chain CH_2 def
39	1388.9	ring breathing + $C7H_2$ twi	1393.3	ring breathing + $C7H_2$ twi
40	1413.6	$C7H_2$ $C9H_2$ wag	1416.7	$C7H_2$ wag
41	1443.7	chain CH_2 wag	1445.1	Chain CH_2 wag
42	1450.6	ring asym str + $C7H_2$ twi + $C6H_3$ def	1456.1	ring asym str + $C7H_2$ twi + $C6H_3$ def
43	1472.7	$C10H_3$ def (umbrella)	1473.0	$C10H_3$ def (umbrella)
44	1490.9	ring asym str + $C6H_3$ def (umbrella)	1491.1	ring asym str + $C6H_3$ def (umbrella)
45	1505.4	$C6H_3$ def (umbrella)	1504.8	$C6H_3$ def (umbrella)
46	1534.6	$C6H_3$ def	1531.8	$C8H_2$ def (sci)
47	1539.1	$C7H_2$ + $C8H_2$ bend (sci)	1534.5	$C6H_3$ def
48	1545.1	chain CH_2 bend (sci)	1541.3	$C7H_2$ bend (sci)
49	1554.8	$C7H_2$ + $C8H_2$ + $C10H_2$ bend (sci)	1549.0	$C8H_2$ + $C9H_2$ + $C10H_2$ bend (sci)
50	1559.8	$C10H_3$ def	1559.5	$C10H_3$ def
51	1562.7	$C6H_3$ def	1562.2	$C6H_3$ def
52	1566.6	chain CH_2 bend (sci)	1565.4	$C8H_2$ + $C9H_2$ + $C10H_2$ bend (sci)
53	1620.5	C4-C5 ring str + C4-H + C5-H ipl sym bend	1618.2	C4-C5 ring str + C4-H + C5-H ipl sym bend
54	1645.7	C2-N ring asym str + C2-H ipl bend	1644.3	C2-N ring asym str + C2-H ipl bend
55	3120.7	$C8H_2$ + $C9H_2$ iph str (sym)	3113.1	$C8H_2$ + $C9H_2$ iph str (sym)
56	3128.6	$C8H_2$ + $C9H_2$ ooph str (sym)	3126.5	$C8H_2$ + $C9H_2$ ooph str (sym)
57	3135.6	$C10H_3$ iph str (sym)	3136.1	$C10H_3$ iph str (sym)
58	3160.9	$C7H_2$ iph str (sym)	3162.8	$C7H_2$ iph str (sym) + $C8H_2$ + $C9H_2$ ooph str
59	3164.3	$C6H_3$ iph str (sym)	3164.3	$C6H_3$ iph str (sym)
60	3171.6	$C8H_2$ + $C9H_2$ ooph str (asym)	3165.5	$C7H_2$ sym str + $C8H_2$ + $C9H_2$ str (asym)
61	3190.6	$C8H_2$ + $C9H_2$ ooph str (asym)	3189.4	$C8H_2$ + $C9H_2$ ooph str (asym)
62	3229.5	$C10H_3$ ooph str (asym)	3230.7	$C10H_3$ ooph str (asym)
63	3232.0	$C7H_2$ ooph str (asym)	3234.2	$C7H_2$ ooph str (asym)
64	3240.4	$C10H_3$ ooph str (sym)	3240.1	$C10H_3$ ooph str (sym)
65	3278.6	$C6H_3$ ooph str (asym)	3278.6	$C6H_3$ ooph str (asym)

66	3286.3	$C6H_3$ ooph str (sym)	3286.4	$C6H_3$ ooph str (sym)
67	3359.7	C3-H C4-H ooph str (asym)	3360.7	C3-H C4-H ooph str (asym)
68	3363.0	C2-H str	3361.9	C2-H str
69	3377.4	C3-H C4-H iph str (sym)	3378.5	C3-H C4-H iph str (sym)

*Key of approximate group vibrations: asym = asymmetric, bend = angle bending (scissoring), breathing = all ring bonds iph, def = more complicated deformation of skeleton, ipl = in plane, iph = in phase (symmetric), oopl = out of ring plane, ooph = opposite motion, out of phase (asymmetric), ring = imidazole core, rot = ring rotation, as a wheel, with carbon H atoms, rock = rocking (like V to *V* by rotation around an axis out of the paper), sci = non-connected scissoring, str = bond stretching, sym = symmetric, tor = torsion around specified bond, twi = twisting of CH_2 group or chain, wag = wagging (like V to v by rotation around an axis in the paper, →).

Table 2. Experimentally observed Raman spectral bands for two common $[C_4C_1Im]^+$ ionic liquids, given in cm^{-1}, and approximate assignments.

ν /cm^{-1}		Assignments*
$[C_4C_1Im][PF_6]$	$[C_4C_1Im][BF_4]$	
498	500	N-C7 opl bend + N-C7-C8-C9 angles bend (GA12)
568		$\nu_2(PF_6^-)$ stretching
601	601	N-C6 N-C7 iph str + ring oopl def + $C8H_2$ rock + N-C7-C8 bend. (GA13)
624	625	ring def (C2-H oopl bend) + N-C6 N-C7 iph str + $C7H_2$ rock + C7-C8-C9 bend (AA14)
656	658	N-C6 str + ring def (N1 and H on C2 oopl ooph departure) + $C8H_2$ wag + N-C7-C8 bend (AA15) + ring def (bend around line NN) + $C8H_2$ rock + N-C7-C8 bend (GA15)
698	699	N-C6 N-C7 ooph str + ring ipl def + $C8H_2$ rock + C7-C8 tor (GA16)
730 ? hidden	~735	N-C6 N-C7 ooph str + ring ipl def + N-C7-C8 and C7-C8-C9 bend (AA17)
741		$\nu_1(PF_6^-)$ stretching

*Key for descriptions of approximate group vibrations, see Table 1; AA and GA mode numbers given in parentheses.

Table 3. Selected vibrational modes as determined in MP2 calculations for the $[C_4C_1Im]^+$ cation in AA and GA conformation. Given are the predicted wavenumber, relative IR and Raman intensities as well as descriptions of the selected modes {46}.

$[C_4C_1Im]^+$ cation in AA conformation				Approx. Description*
Mode	ν/ cm^{-1}	IR intensity / km $mole^{-1}$	Raman activity / $Å^4$ amu^{-1}	
13	620	0.52	1.34	ring oopl def + $C7H_2$ rock + C7-C8-C9 bend
14	636	9.40	2.59	ring def (C2-H oopl bend) + N-C6 N-C7 iph str + $C7H_2$ rock + C7-C8-C9 bend
15	670	12.23	1.36	N-C6 str + ring def (N1 and H on C2 oopl ooph departure) + $C8H_2$ wag + N-C7-C8 bend
17	749	13.06	2.13	N-C6 N-C7 ooph str + ring ipl def + N-C7-C8 and C7-C8-C9 bend
$[C_4C_1Im]^+$ cation in GA conformation				Approx. Description*
Mode	ν/ cm^{-1}	IR intensity / km $mole^{-1}$	Raman activity /$Å^4$ amu^{-1}	
12	504	0.65	1.19	N-C7 opl bend + N-C7-C8-C9 angles bend
13	604	1.46	5.99	ring ipl def + $C8H_2$ rock + N-C7-C8 bend
14	623	2.82	0.36	ring def (C2-H C4-H iph oopl bend) + $C8H_2$ rock + N-C7-C8 bend
15	663	15.62	0.56	ring def (bend around line NN) + $C8H_2$ rock + N-C7-C8 bend

16	713	6.65	2.15	N-C6, N-C7 ooph str + ring ipl def + $C8H_2$ rock + C7-C8 tor

* For key of approximate group vibrations, see Table 1.

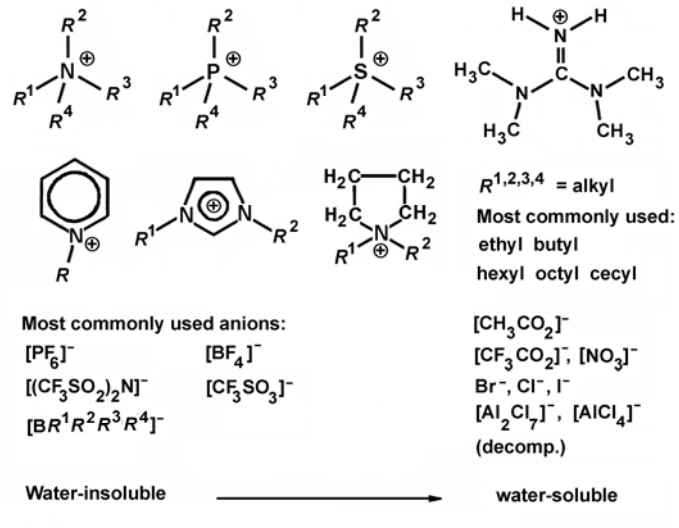

Figure 1. Common ionic liquids include ammonium, phosphonium, sulfonium, guanidinium, pyridinium, imidazolium, and pyrrolidinium cations and Cl^-, Br^-, $[BF_4]^-$, $[PF_6]^-$, $[TfO]^-$ (trifluoromethane-sulfonate) and $[Tf_2N]^-$ (bis(trifluoromethylsulfonyl)imide) anions. However use of nomenclature vary among researchers. We prefer the notation $[C_4C_1Im]^+$ for 1-butyl-3-methyl-imidazolium in stead of $[bmim]^+$, $[BMIM]^+$ or others. Similarly, e.g. we will call the bis(trifluoromethanesulfonyl)imide $[(CF_3SO_2)_2N]^-$ anion $[Tf_2N]^-$ (Tf is a short-hand notation for triflate); other acceptable abbreviated names occur in recent literature.

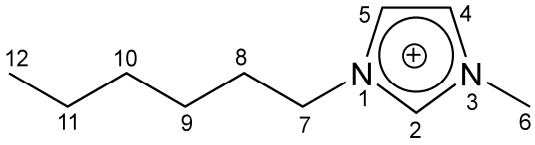

Figure 2. Numbering scheme in the 1- hexyl -3-methylimidazolium cation, $[C_6C_1Im]^+$, showing the three ring protons H2, H4, and H5.

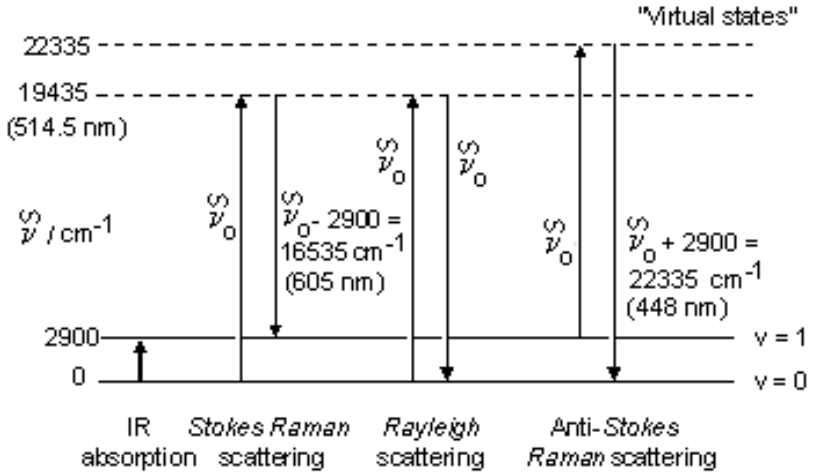

Figure 3. The relationships between infrared absorption, Rayleigh and Raman scattering:

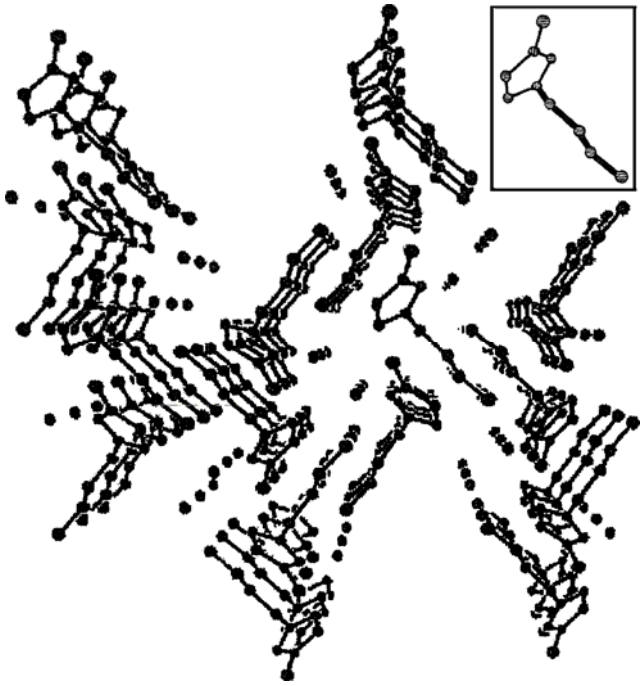

Figure 4. Crystal structure of $[C_4C_1Im]Cl$ ”Crystal (1)” viewed along the ***a*** axis. Only carbon atoms, nitrogen atoms, and chloride anions are shown. The *anti-anti* (AA) conformation of the $[C_4C_1Im]^+$ cation is shown in the inset. The butyl group C-C bonds are shown as thick bars. Note that the cations and chloride anions form characteristic columns along the crystal ***a*** axis (figure adapted from Hamaguchi et al. {50}).

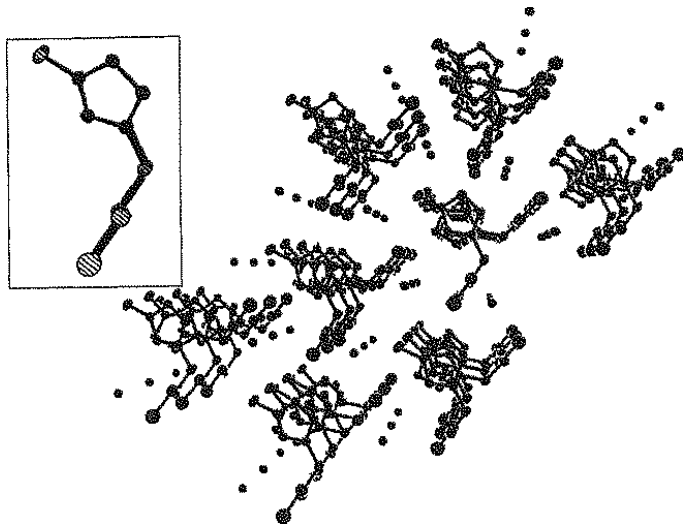

Figure 5. Crystal structure of $[C_4C_1Im]Br$ viewed in the direction of the ***a*** axis. Only carbon atoms, nitrogen atoms, and bromide anions are shown. The *gauche-anti* (GA) conformation of the $[C_4C_1Im]^+$ cation is shown in the inset. The butyl group C-C bonds are shown as thick bars (figure adapted from Hamaguchi et al. {50}).

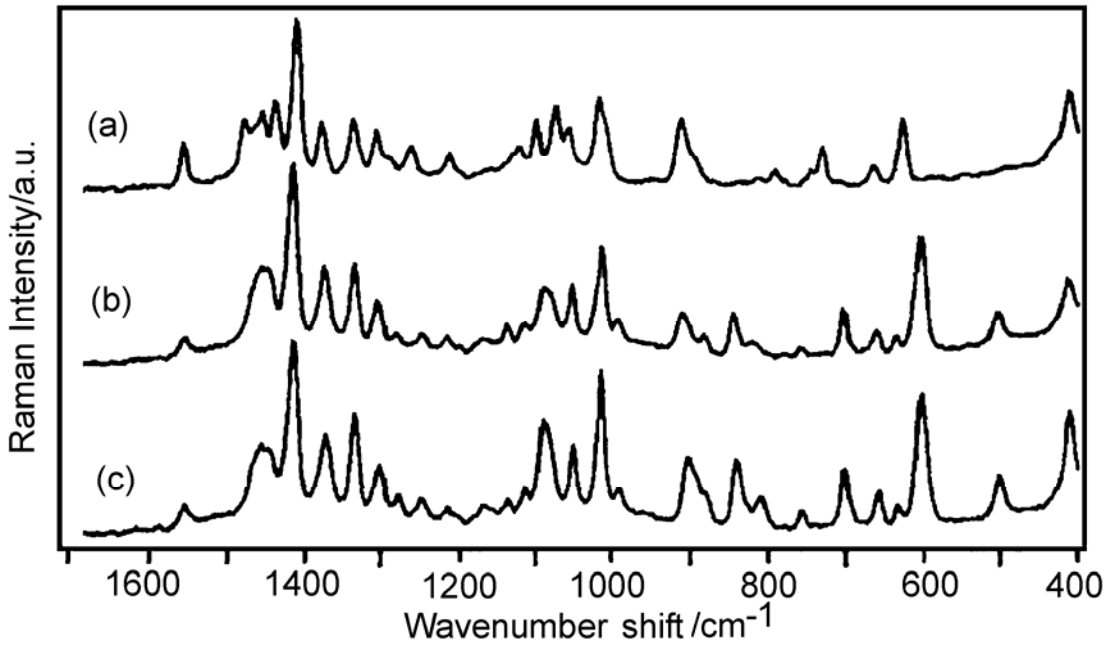

Figure 6. Raman spectra of (a) $[C_4C_1Im]Cl$ "Crystal (1)", (b) $[C_4C_1Im]Cl$ "Crystal (2)", and (c) $[C_4C_1Im]Br$ crystals. (a) differs from (b) and (c) (figure has been adapted from Hamaguchi et al. {50}).

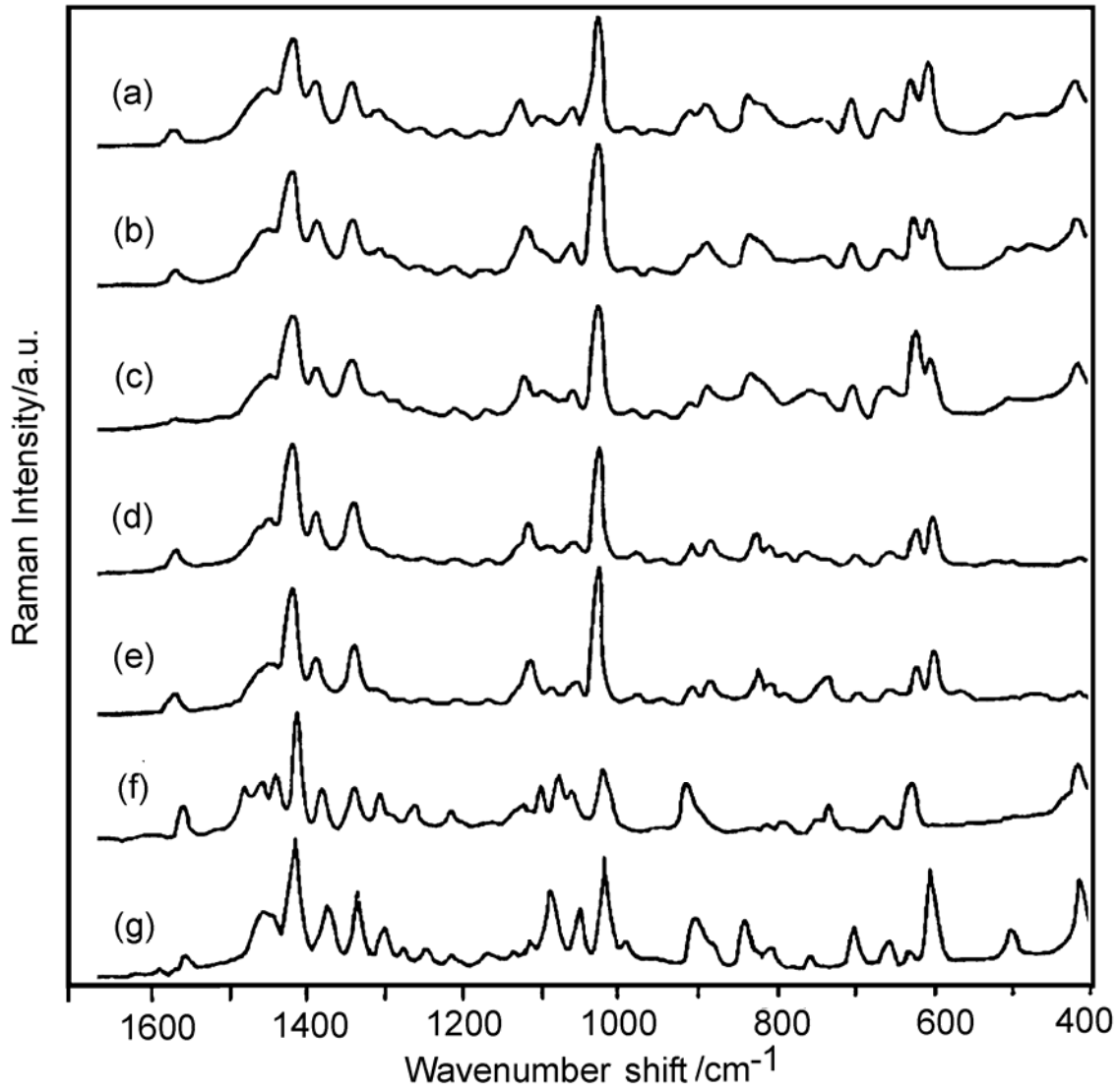

Figure 7. Raman spectra of liquid $[C_4C_1Im]X$, where X = C1 (a), Br (b), I (c), $[BF_4]$ (d), and $[PF_6]$ (e). *The anion bands in (d) and (e) have been deleted* {50}. Spectra of $[C_4C_1Im]Cl$ "Crystal (1)" and crystalline $[C_4C_1Im]Br$, respectively, are included as (f) and (g), for reference purposes (figure adapted from Hamaguchi et al. {50}).

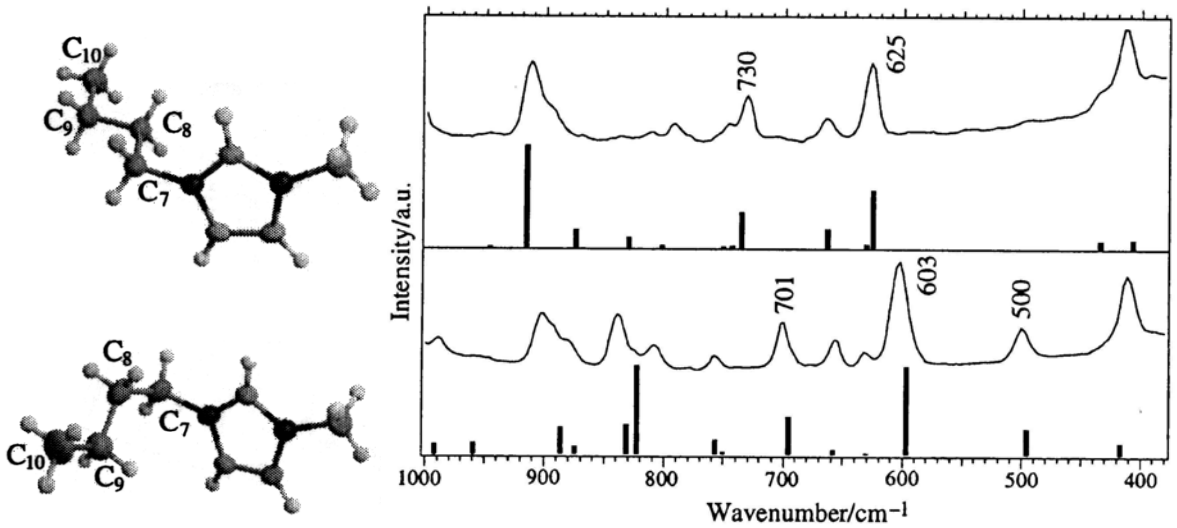

Figure 8. Optimized structures of the $[C_4C_1Im]^+$ cation in the two crystals. Experimental (continuous lines) and calculated Raman spectra (solid vertical bars) of $[C_4C_1Im]Cl$ "Crystal (1)" (above) and $[C_4C_1Im]Br$ (below) are shown (figure has been adapted from Hamaguchi et al. {50}, {70}).

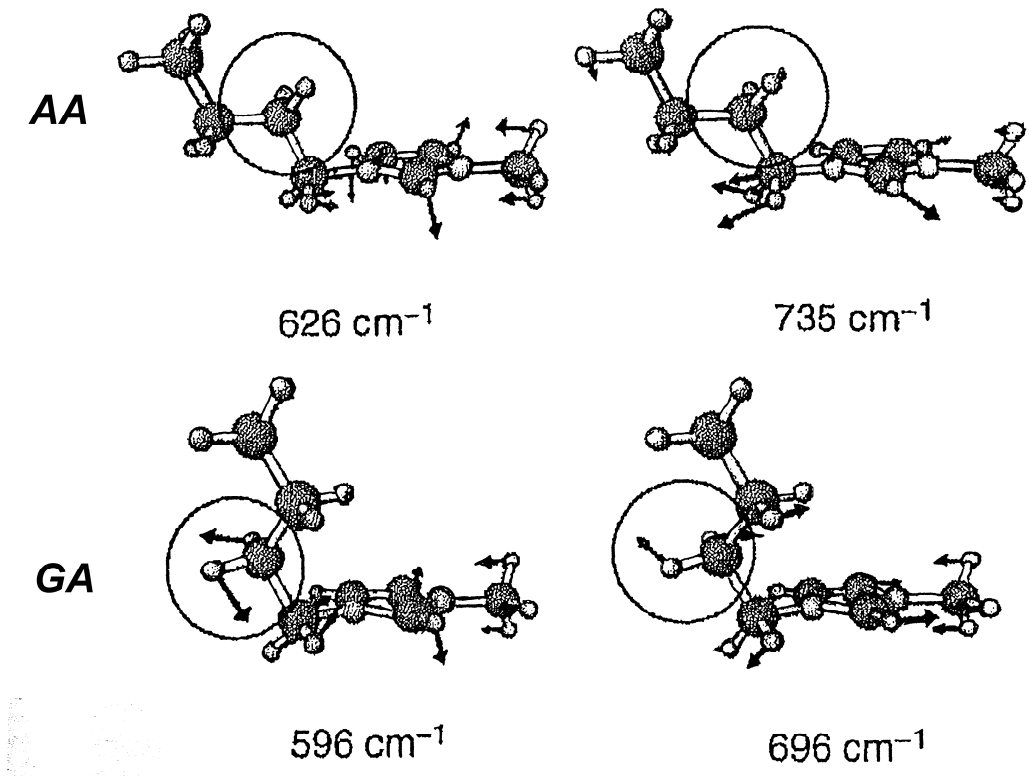

Figure 9. Calculated normal modes of key bands of the AA and GA forms of the $[C_4C_1Im]^+$ cation. The arrows indicate vibrational amplitudes of atoms. The C8 methylene group is surrounded by a circle. Obviously it appears that the CH_2 rocking vibration is coupled to the ring modes only for the GA conformer, thereby lowering the frequencies. Graphics adapted from Hamaguchi et al. {50}.

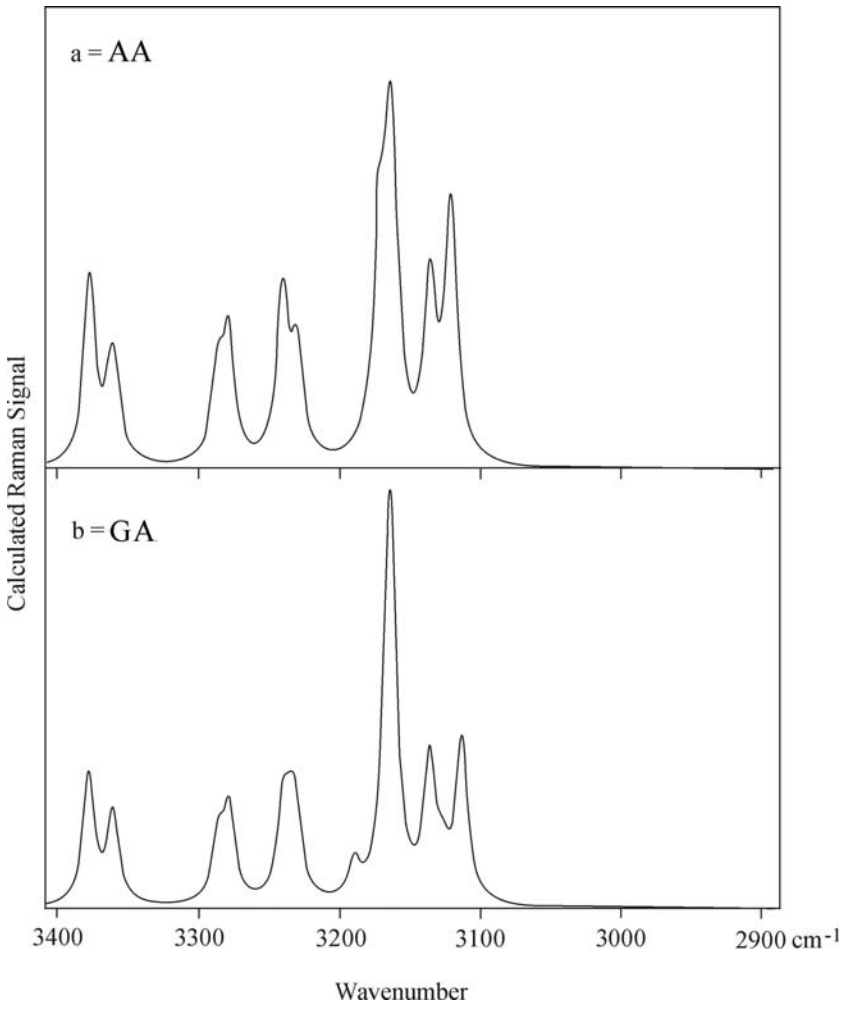

Figure 10. Calculated Raman spectra of two conformers of the $[C_4C_1Im]^+$ cation in the range between 3400 and 2900 cm^{-1}. a: The *anti-anti* conformer; b: The *gauche-anti* conformer. Data from {72}.

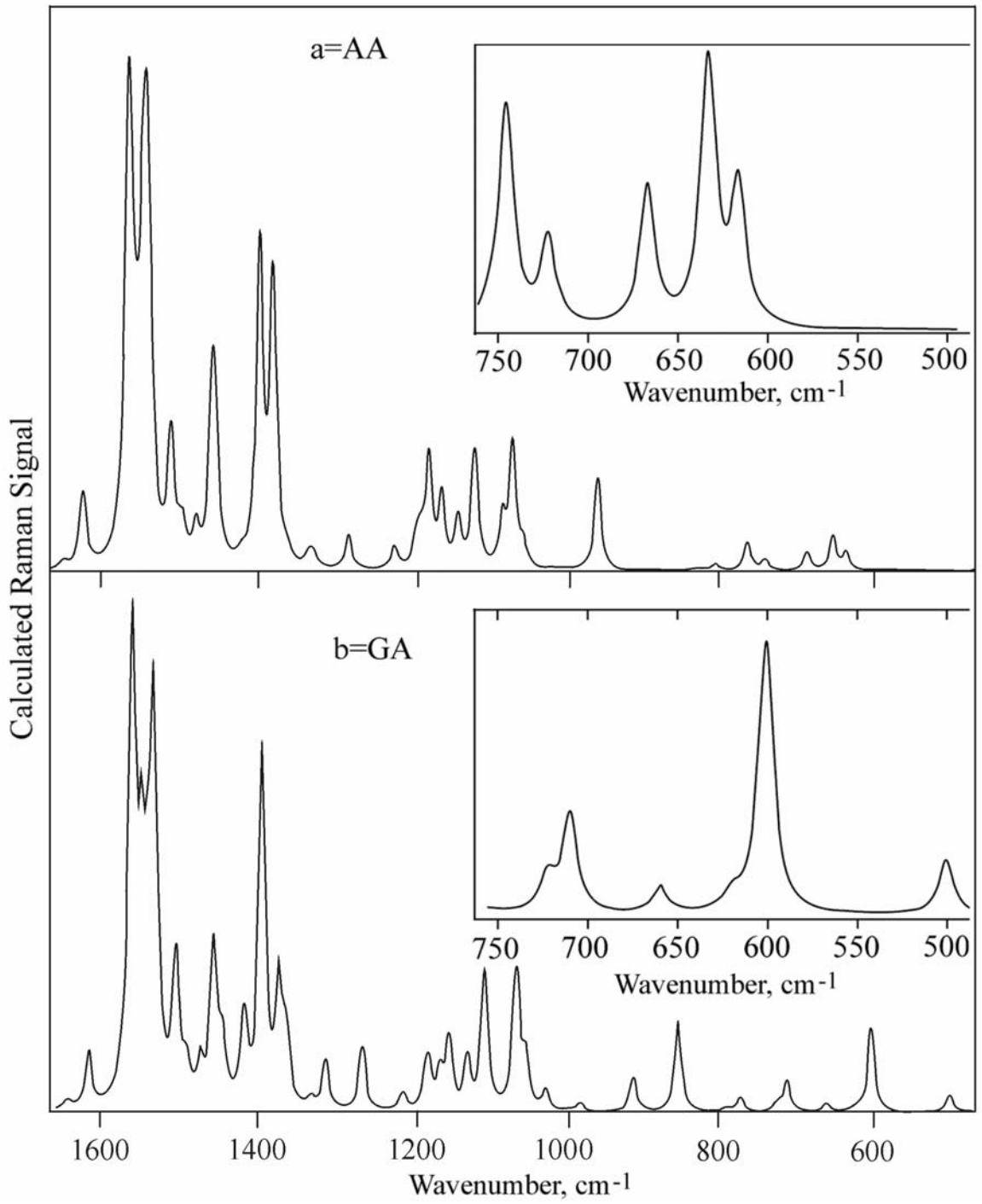
a=AA
b=GA
Calculated Raman Signal
750
700
650
600
550
500
Wavenumber, cm-1
1600
1400
1200
1000
800
600
Wavenumber, cm-1

Figure 11. Calculated Raman spectra of two conformers of the $[C_4C_1Im]^+$ cation in the range between 1650 and 400 cm^{-1}. a: The *anti-anti* conformer; b: The *gauche-anti* conformer. Data from {46} and {72}.

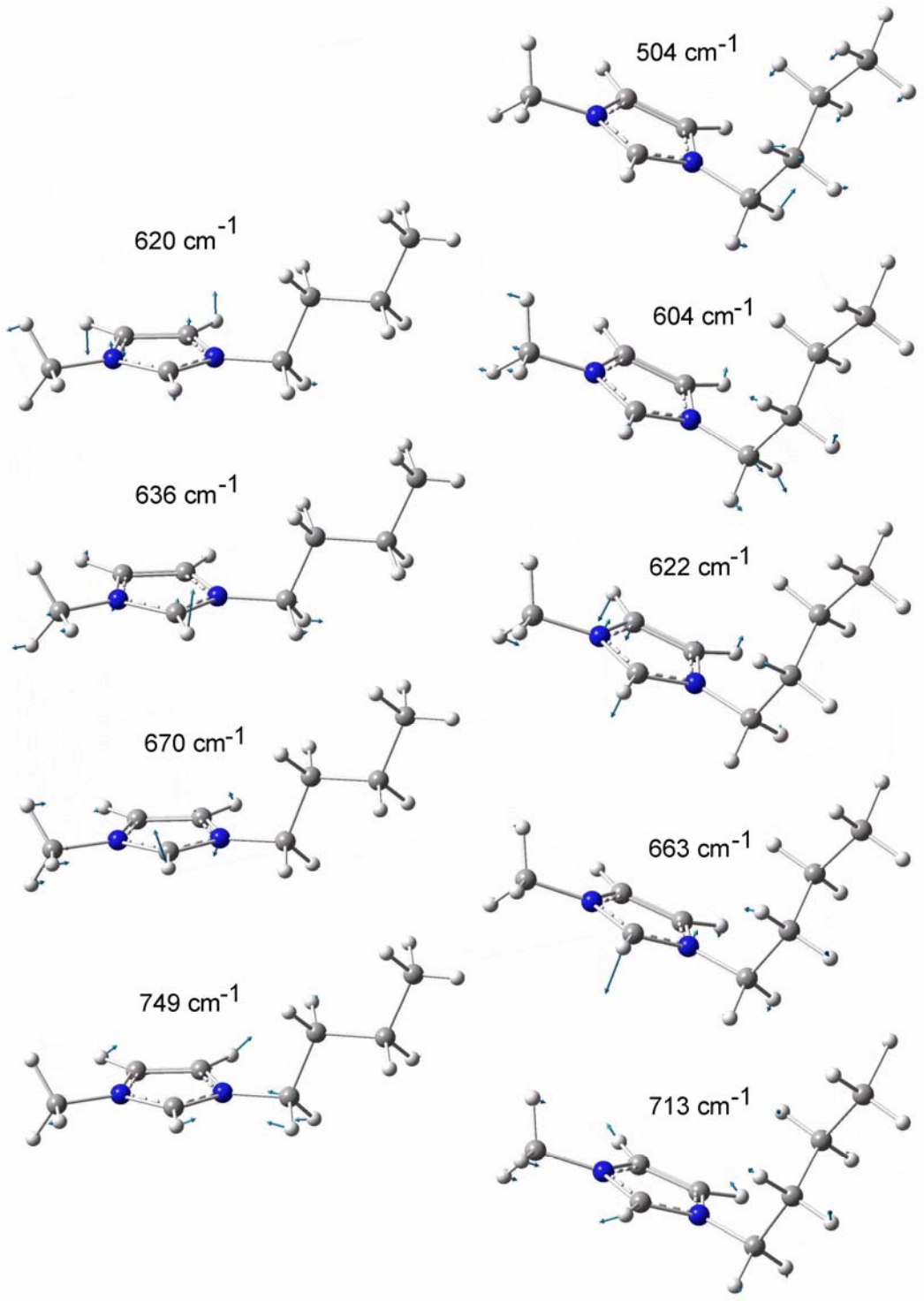
504 cm-1
620 cm-1
604 cm-1
636 cm-1
622 cm-1
670 cm-1
663 cm-1
749 cm-1
713 cm-1

Figure 12. Some of our calculated normal modes of certain bands of the AA and GA forms of the $[C_4C_1Im]^+$ cation. The arrows indicate vibrational amplitudes of atoms. As found by Hamaguchi et al. {50} also our C8 methylene CH_2 rocking vibration was coupled to the ring modes only for the *gauche-anti* conformer {46} and {72}.

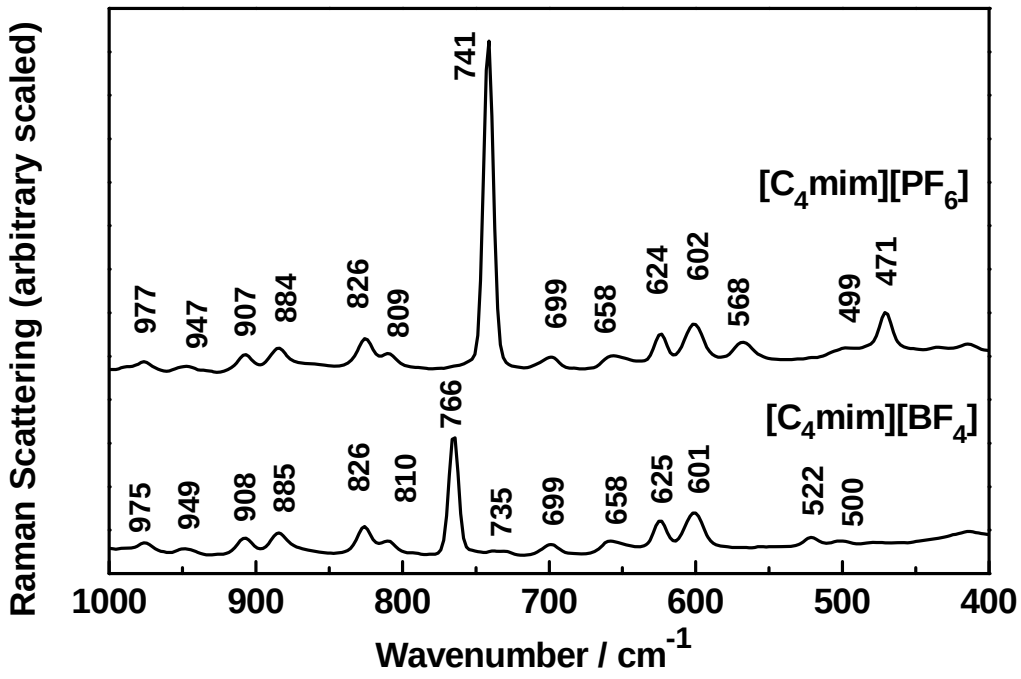

Figure 13. Details of FT-Raman spectra of the $[C_4C_1Im][PF_6]$ and $[C_4C_1Im][BF_4]$ ionic liquids at ~25ºC {72}. Note that the characteristic bands of the AA and GA forms of the $[C_4C_1Im]^+$ cation are present in both melts, as also found e.g. by Hamaguchi et al. {50}.

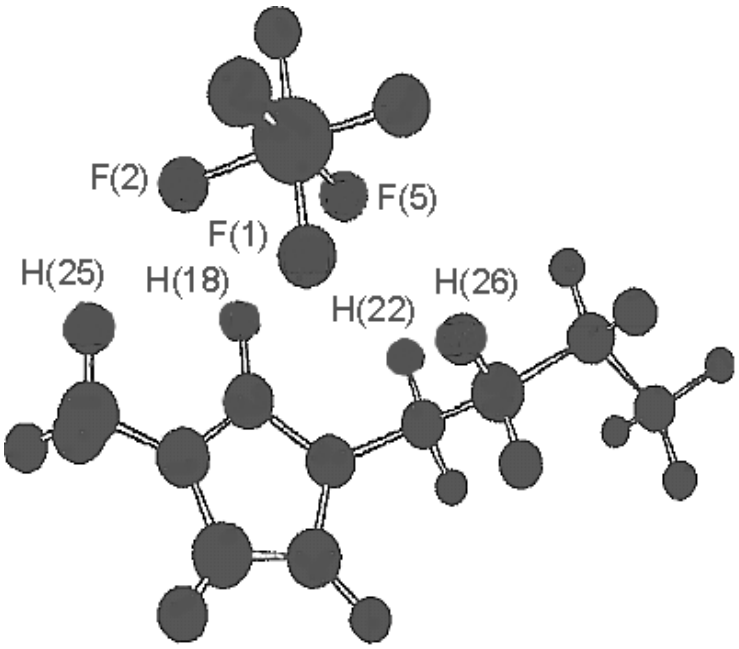

Figure 14. Minimized molecular structure of $[C_4C_1Im][PF_6]$ (B3LYP/6-31G*) {5}. Found hydrogen bonds included: F2-H25 = 2.279 Å; F2-H18 = 2.042 Å; Fl-H18 = 2.441 Å; F5-H18 = 2.070 Å, F5-H22 = 2.419 Å and Fl-H26 = 2.377 Å. Figure adapted from Meng et al. {5}.

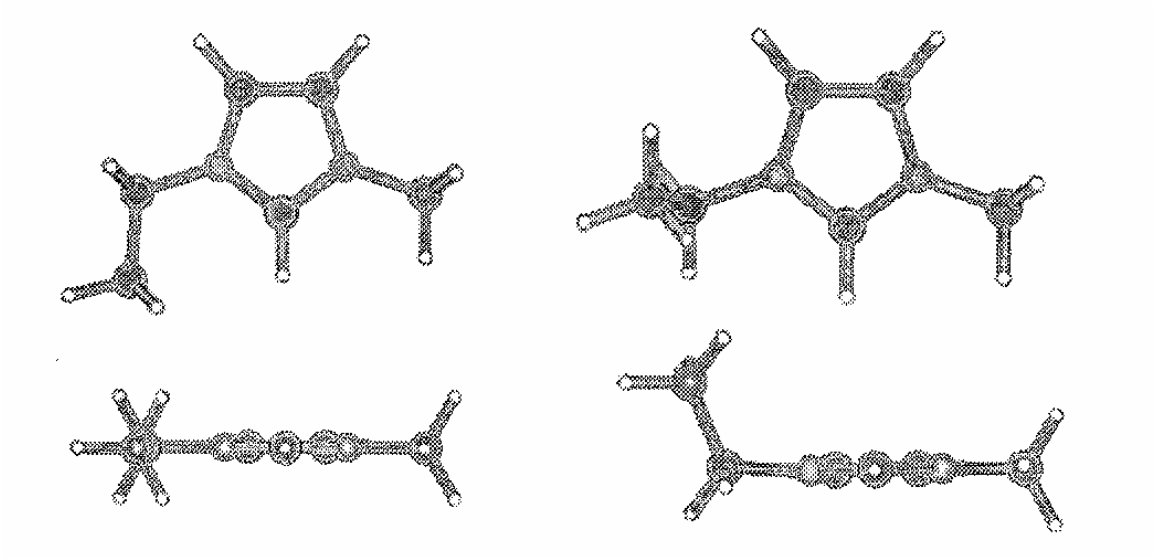

Figure 15. Calculated structures of the $[C_2C_1Im]^+$ cation, showing the two different torsion conformers obtainable by rotation of the ethyl group around the C-N bond relative to the imidazolium ring. Planar (left) and nonplanar (right) rotamers are viewed perpendicular to and along the ring plane. The nonplanar form is known from X-ray structures {69}. Figure adopted from Umebayashi et al. {80}.

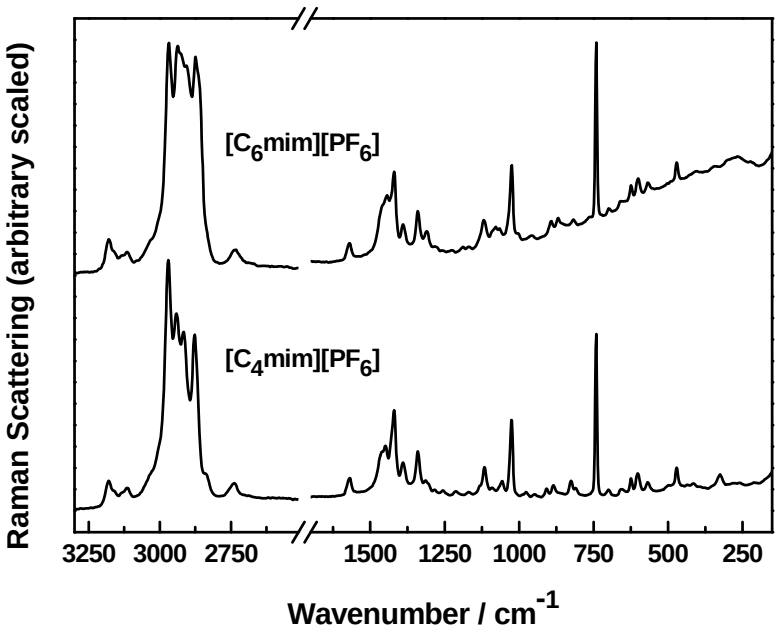

Figure 16. FT-Raman spectra of the $[C_6C_1Im][PF_6]$ and $[C_4C_1Im][PF_6]$ ionic liquids at ~25ºC. Note that the characteristic bands of the AA and GA forms of the $[C_4C_1Im]^+$ cation are very much like the AAAA and GAAA bands from the $[C_6C_1Im]^+$ cation {46}{72}.

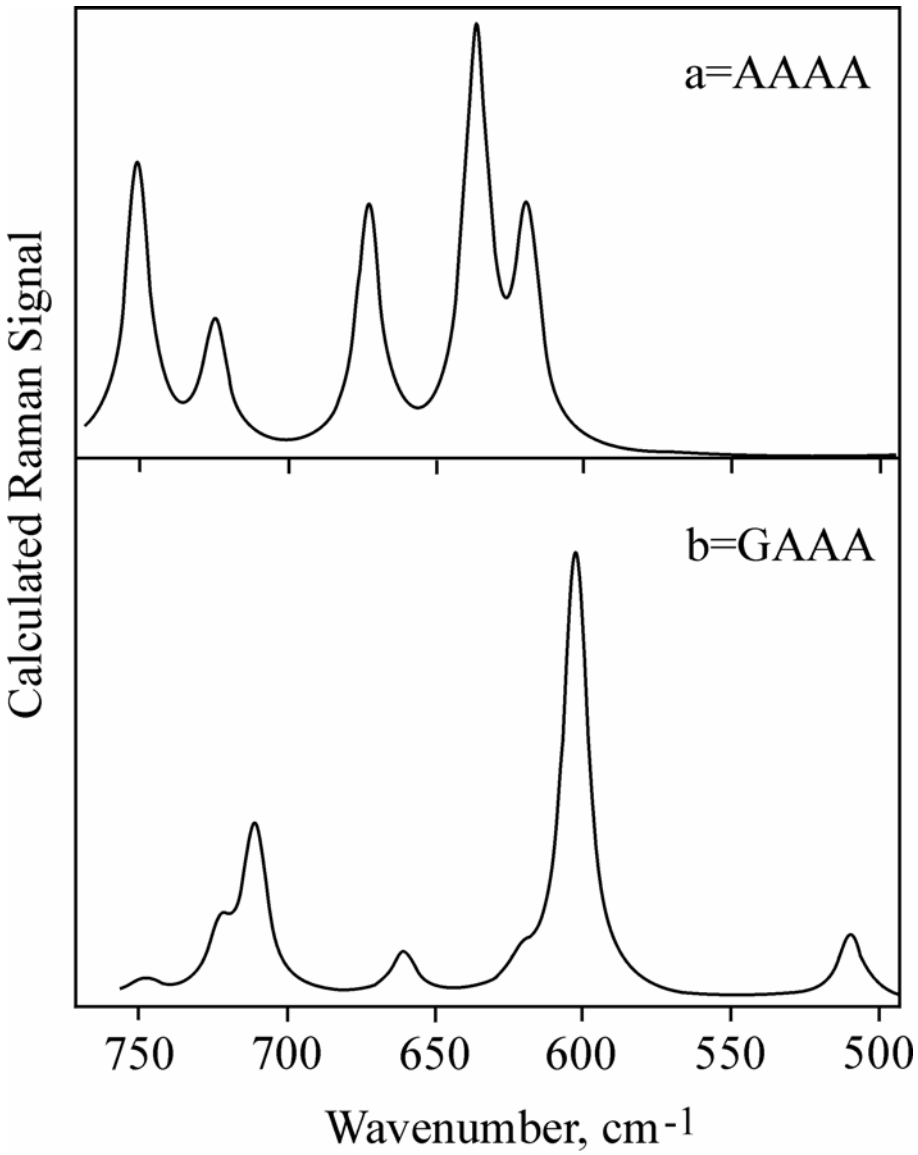

Figure 17. Our calculated Raman spectra of two conformers of the hexyl $[C_6C_1Im]^+$ cation between 750 and 500 cm^{-1}. a: all-anti conformer AAAA; b: gauche-anti-anti-anti GAAA conformer {46}.

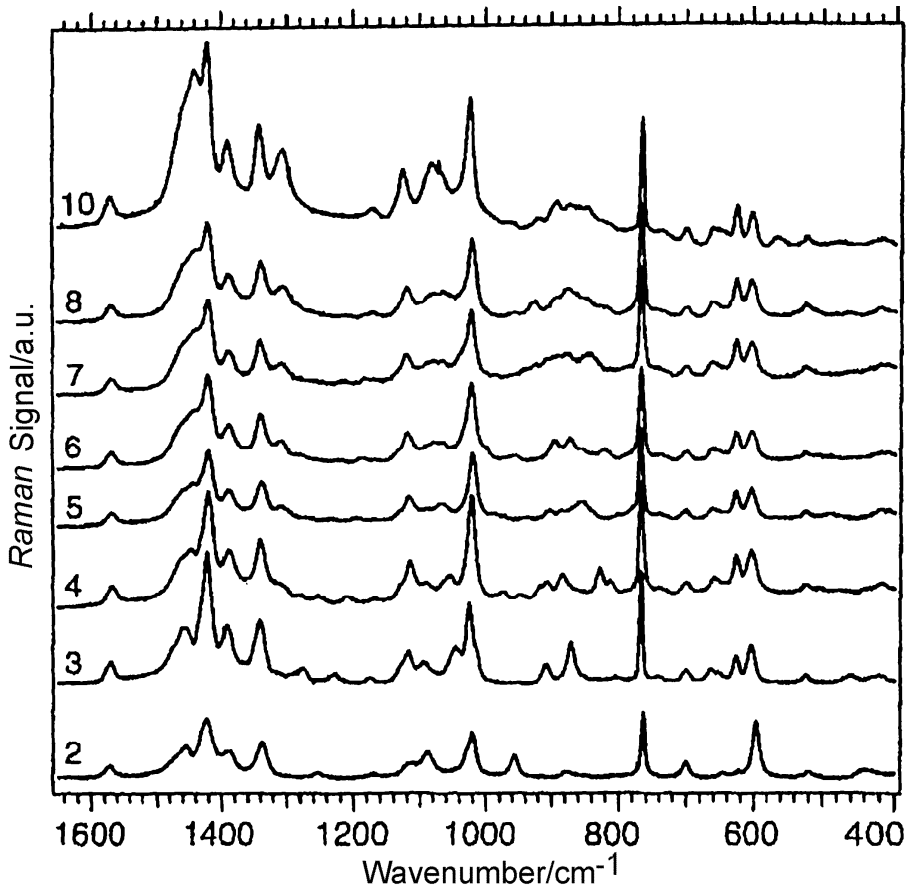

Figure 18. Raman spectra of 1-alkyl-3-methylimidazolium tetrafluoroborate liquids, $[C_nC_1Im][BF_4]$ for n = 10, 8, 7, 6, 5, 4, 3, and 2. The figure has been adapted from Hamaguchi et al. {50}.

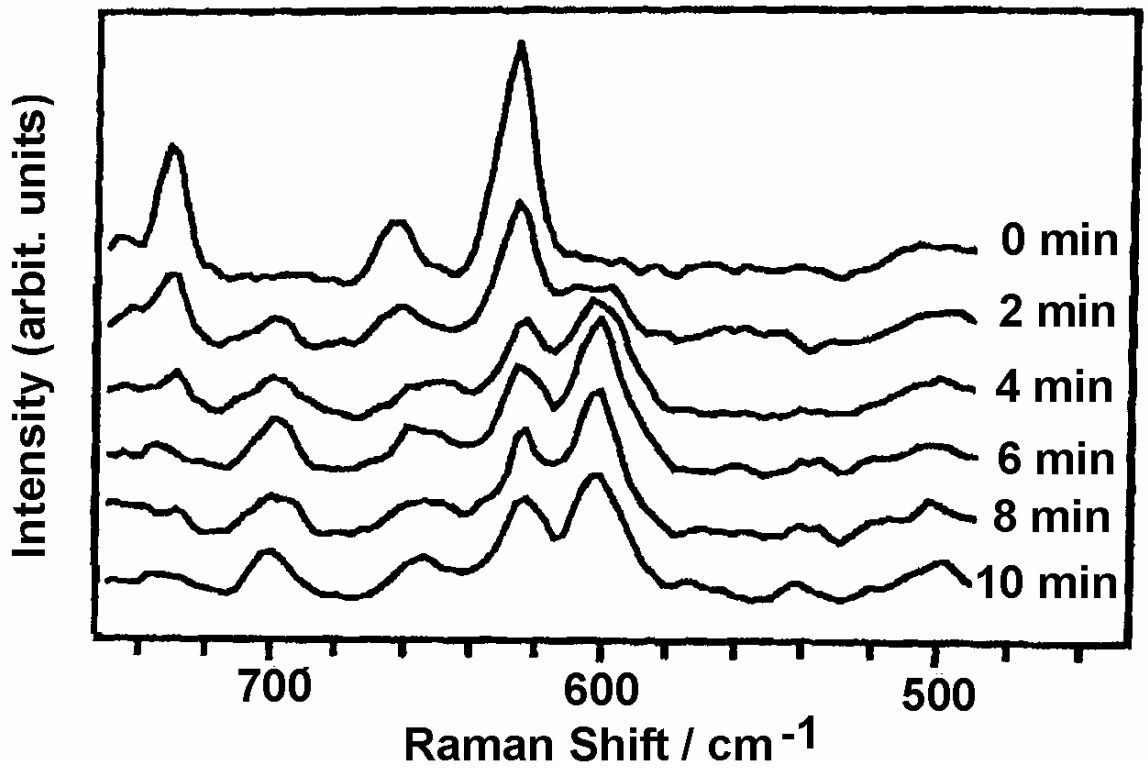

Figure 19. Time-resolved Raman spectra of the melting and thermal equilibration process at 72°C for a $[C_4C_1Im]Cl$ "Crystal (1)" sample. The figure has been adapted from Hamaguchi et al. {50}, {86}.

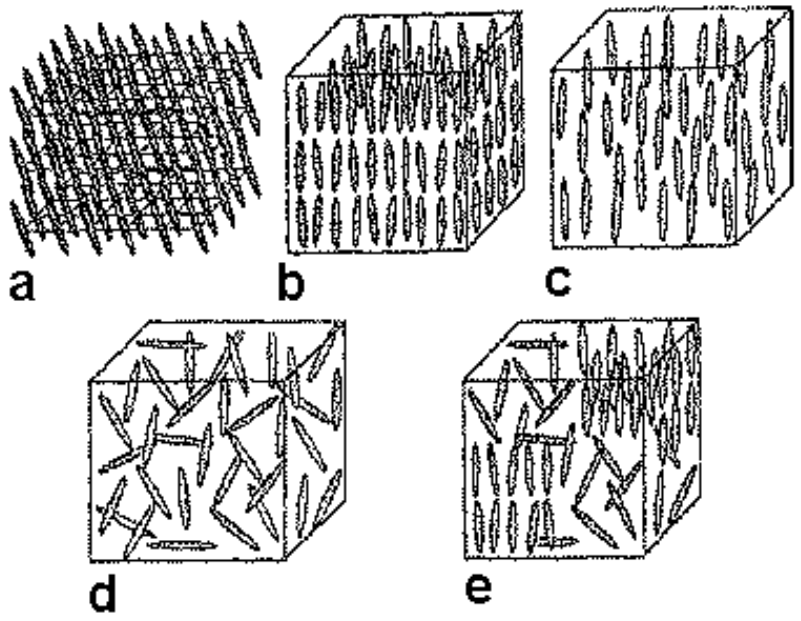

Figure 20. Conceptual structure of ionic salt crystals and liquids: a = crystal, b and c = liquid crystals, d = liquid, e = ionic liquid, according to the model of Hamaguchi and Ozawa {50}. Figure adapted from Hamaguchi et al. {50}.

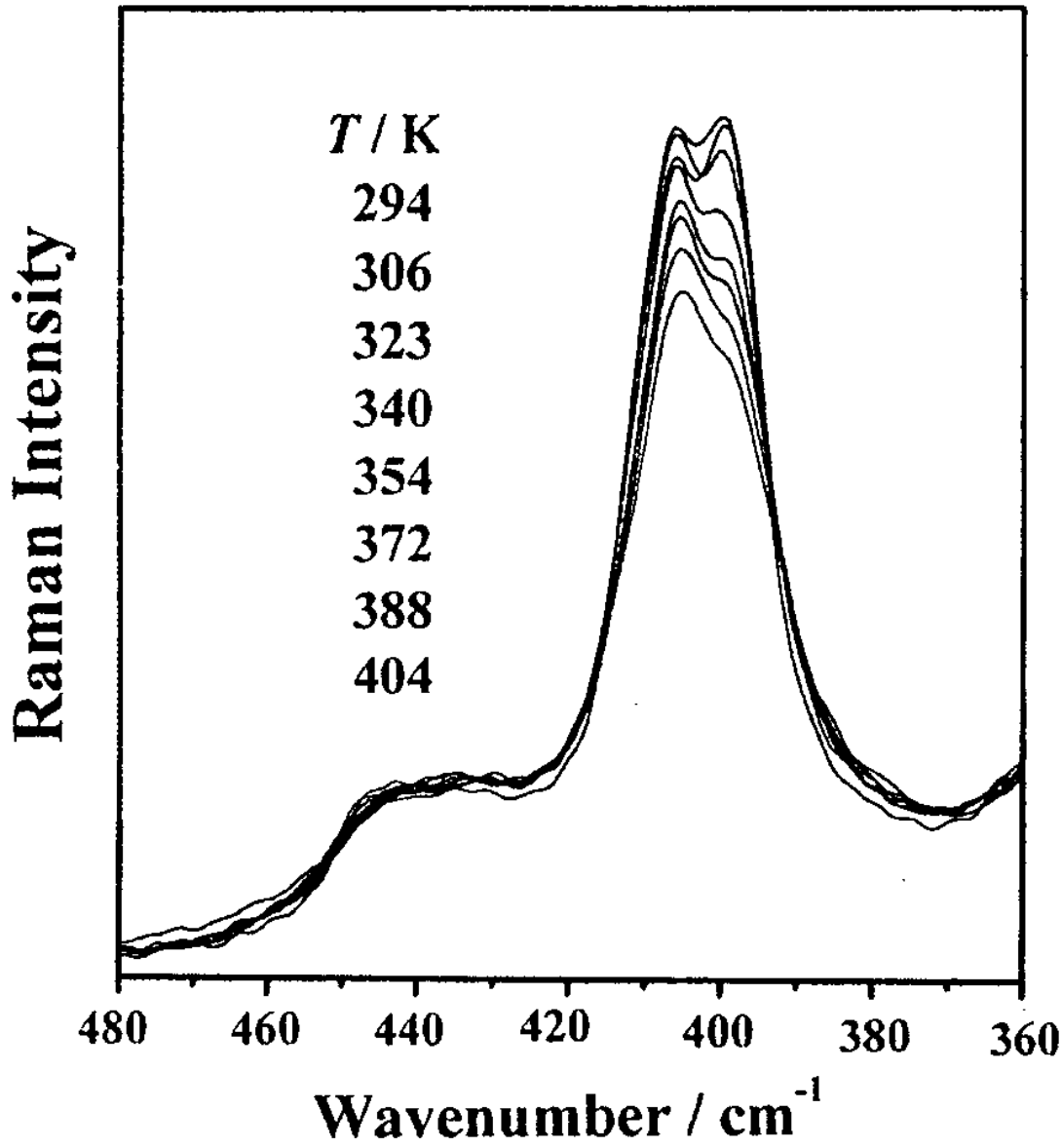

Figure 21. Raman spectra of the 1-ethyl-3-methylimidazolium liquid $[C_2C_1Im][Tf_2N]$ showing the temperature dependent SO_2 wagging bands at ~398 and ~407 cm^{-1}. According to Fujii et al. {108} the bands arise from different conformers of the $[Tf_2N]^-$ ion, known also from crystal structures {109}. Figure adapted from Fujii et al. {108}.

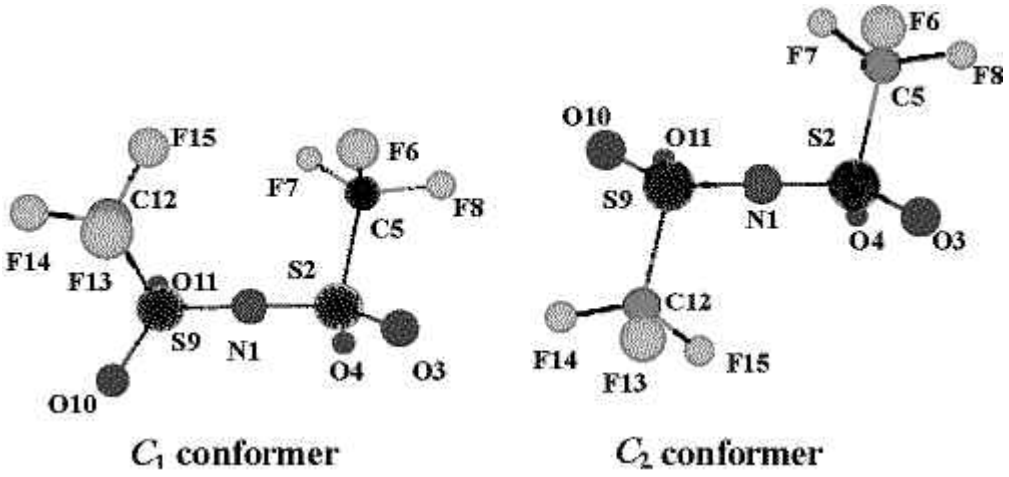

Figure 22. Different conformers of symmetry C_1 and C_2 of the $[Tf_2N]^-$ ion, as determined by Fujii et al. {108} by means of DFT calculations for the 1-ethyl-3-methylimidazolium liquid $[C_2C_1Im][Tf_2N]$. Figure adapted from Fujii et al. {108}.

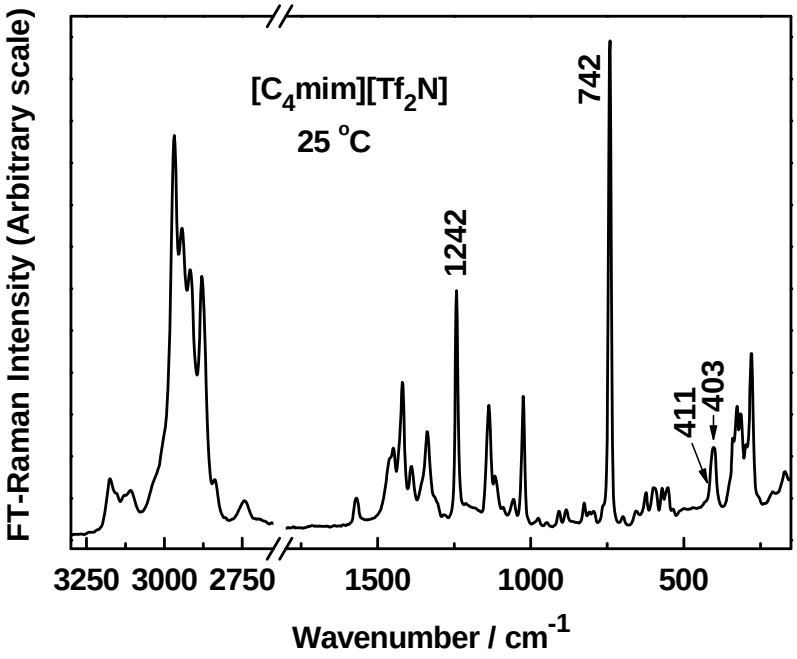

Figure 23. Our Raman spectrum of liquid $[C_4C_1Im][Tf_2N]$. Apparently the splitting between the two conformation sensitive bands for the $[Tf_2N]^-$ ion, near ~400 cm^{-1}, is not so large in this liquid as for the 1-ethyl $[C_2C_1Im][Tf_2N]$ case {108}. The CF_3 symmetric stretching and deformation bands are seen at 1242 and 742 cm^{-1}. The AA/GA conformational equilibrium bands at 500-700 cm^{-1} discussed in relation with Fig. 7 can also be weakly seen {72}.

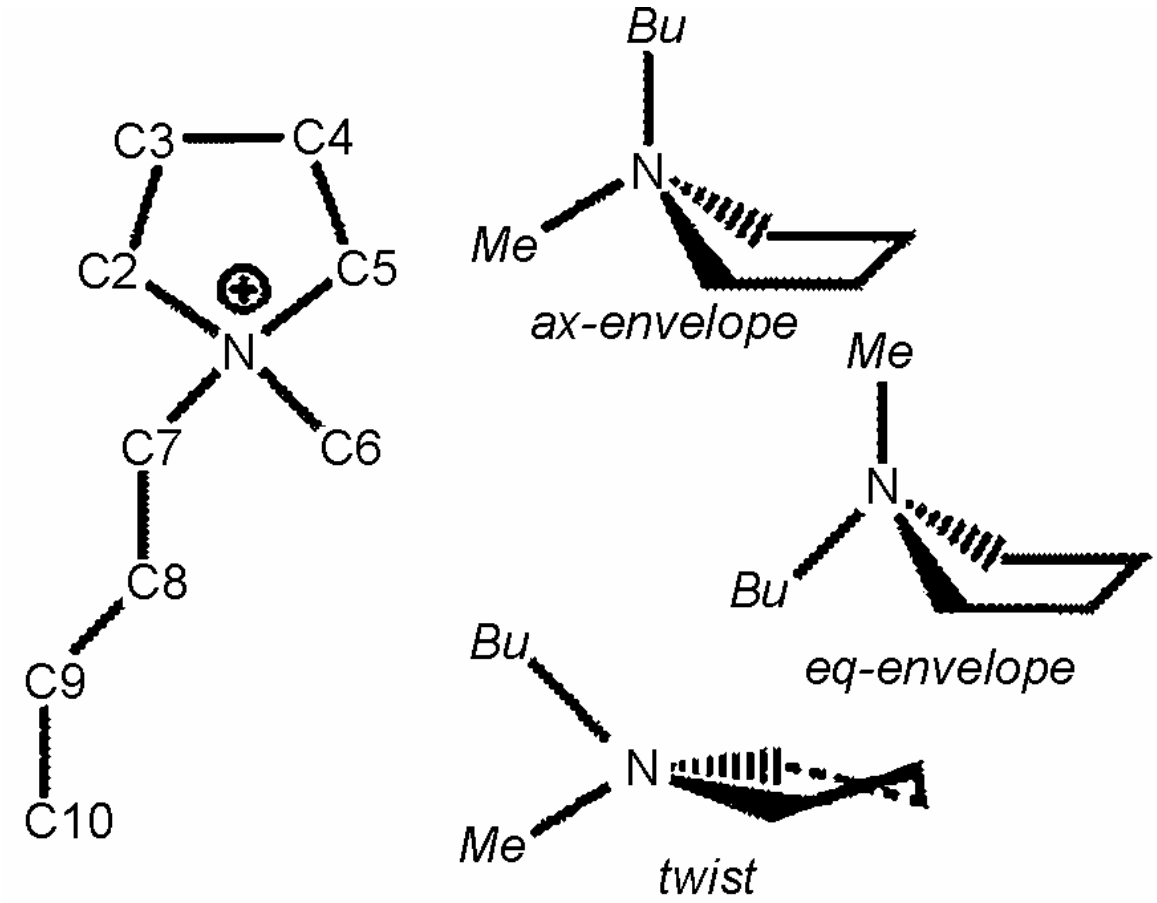

Figure 24. Structure and conformations of N-butyl-N-methylpyrrolidinium (or 1-butyl-1-methylpyrrolidinium or $[P14]^+$ or $[bmpy]^+$; several names are used). In $[P14]^+$ P denotes pyrrolidinium and the digits the number of carbon atoms in radicals R^1 and R^2. Also, the ion is commonly called $[bmpy]^+$ (N is atom number 1). The ring of the $(CH_2)_4NR^1R^2$ pyrimidinium ion is not planar and has two stable (*twist* and *envelope*) forms.

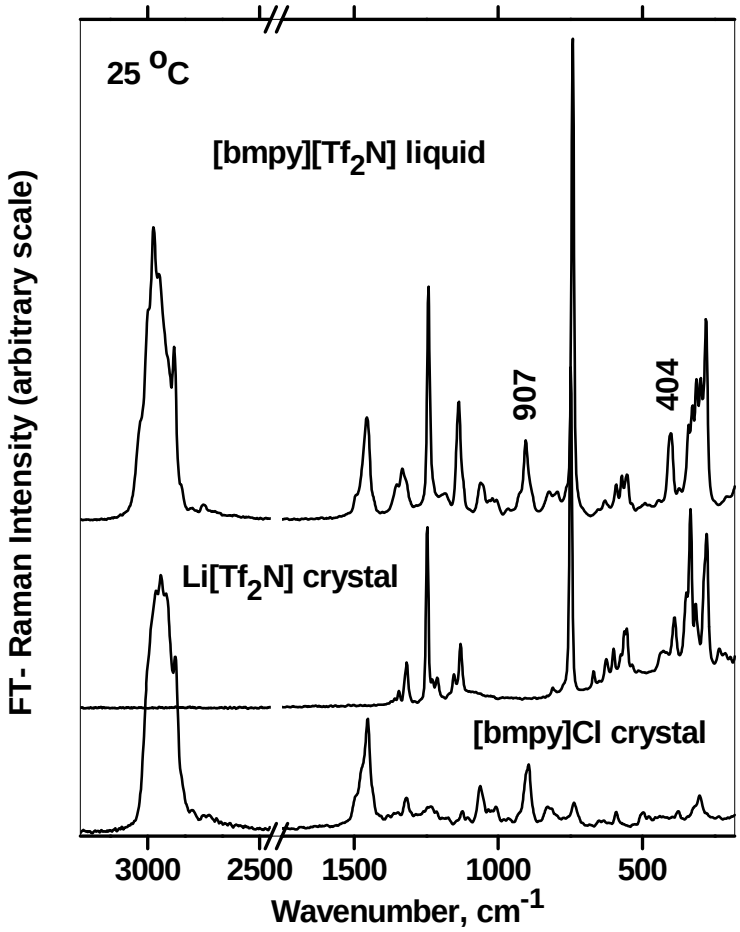

Figure 25. Experimental FT-Raman spectra for the [bmpy][Tf_2N] liquid (also called [P14][TFSI] {113}), showing that the spectum (top) at room temperature essentially consists of bands from both the [Tf_2N]$^-$ anion (middle) and the [bmpy]$^+$ cation (bottom) (shifted conveniently). The Li^+ and Cl^- do not contribute bands directly in the liquid but have influence on the structures of the salts and are interacting with the ions and influencing the conformational equilibria in the IL {72}.

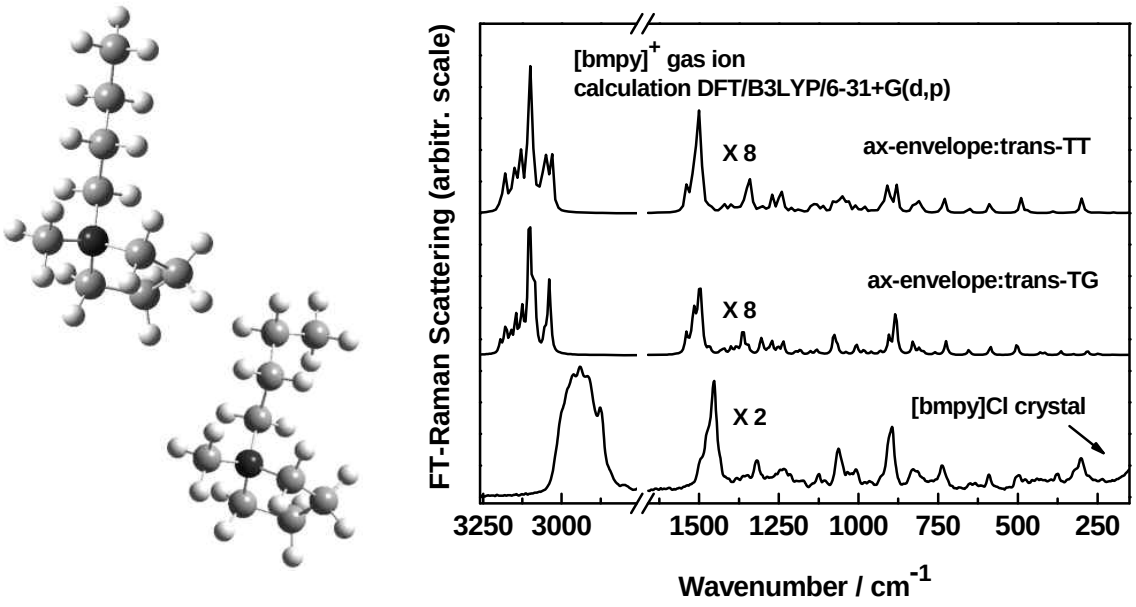

Figure 26. Minimized structures of the so-called *ax-envelope:trans-TT and -TG* confomations of the $[bmpy]^+$ ion in assumed gaseous state calculated {72} at the DFT/B3LYP/6-31+ G (p,d) level. The minimized bond distances and angles had standard magnitudes. The model spectra shown compare well to the experimental FT-Raman spectrum of the $[bmpy]^+$ ion in the solid chloride salt {72}.

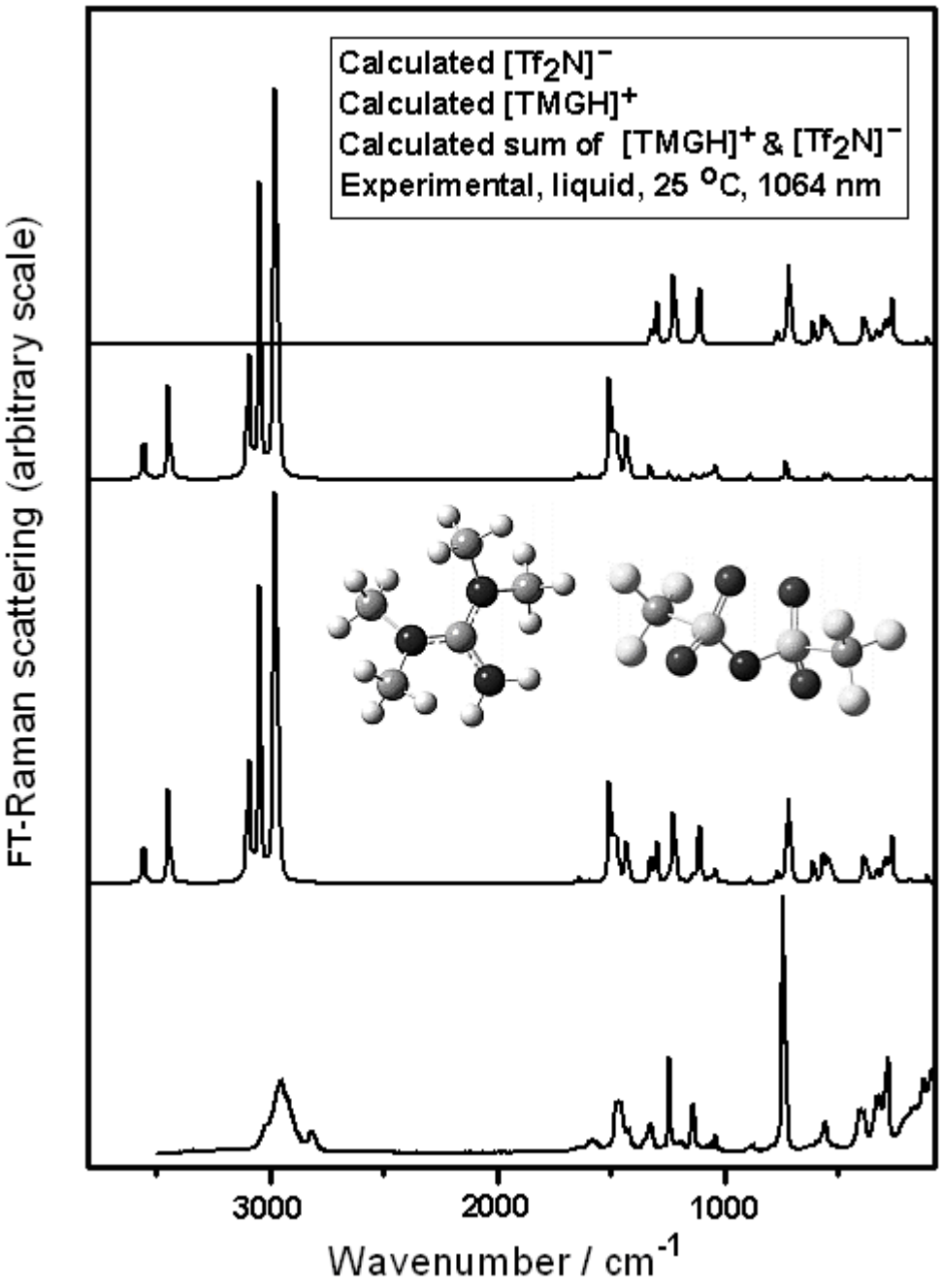

Figure 27. Illustrative example of the power of *ab-initio* methods combined with Raman spectroscopy, applied on the [TMGH][Tf_2N] liquid. The two top spectral curves show calculated Raman spectra of minimized conformers of [Tf_2N]$^-$ and [TMGH]$^+$ at the DFT/B3LYP/6-31G(d) level. The geometries of

the ions are also depicted together with the sum of the spectra, constituting a hypothetical [TMGH][Tf_2N] liquid of non-interacting ions (shifted conveniently). Bottom: the experimental FT-Raman spectrum. Unfortunately measurements exist only below 3500 cm^{-1} {72}.